

1995

A Correlated LM/SEM Method for the Morphological Characterization of Gene Expression in *Xenopus laevis*

Laura Rochmis
College of William & Mary - Arts & Sciences

Follow this and additional works at: <https://scholarworks.wm.edu/etd>



Part of the [Genetics Commons](#), and the [Morphology Commons](#)

Recommended Citation

Rochmis, Laura, "A Correlated LM/SEM Method for the Morphological Characterization of Gene Expression in *Xenopus laevis*" (1995). *Dissertations, Theses, and Masters Projects*. Paper 1539625967. <https://dx.doi.org/doi:10.21220/s2-b414-c286>

This Thesis is brought to you for free and open access by the Theses, Dissertations, & Master Projects at W&M ScholarWorks. It has been accepted for inclusion in Dissertations, Theses, and Masters Projects by an authorized administrator of W&M ScholarWorks. For more information, please contact scholarworks@wm.edu.

**A Correlated LM/SEM Method for the Morphological Characterization
of Gene Expression in *Xenopus laevis***

A Thesis

Presented to

The Faculty of the Department of Biology

The College of William and Mary

In Partial Fulfillment

of the Requirements for the Degree of

Master of Arts

by

Laura Rochmis

1995

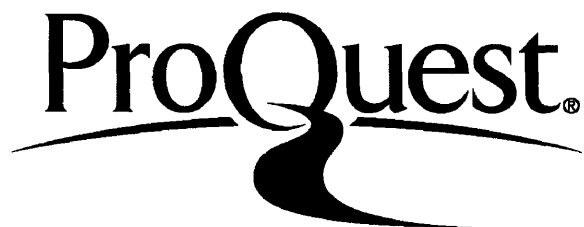
ProQuest Number: 10629425

All rights reserved

INFORMATION TO ALL USERS

The quality of this reproduction is dependent upon the quality of the copy submitted.

In the unlikely event that the author did not send a complete manuscript and there are missing pages, these will be noted. Also, if material had to be removed, a note will indicate the deletion.



ProQuest 10629425

Published by ProQuest LLC (2017). Copyright of the Dissertation is held by the Author.

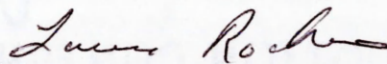
All rights reserved.

This work is protected against unauthorized copying under Title 17, United States Code
Microform Edition © ProQuest LLC.

ProQuest LLC.
789 East Eisenhower Parkway
P.O. Box 1346
Ann Arbor, MI 48106 - 1346

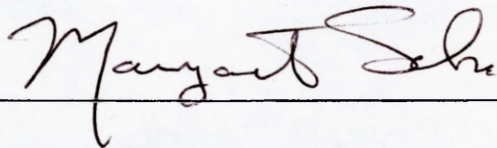
APPROVAL SHEET

This thesis is submitted in partial fulfillment of
the requirements for the degree of
Master of Arts

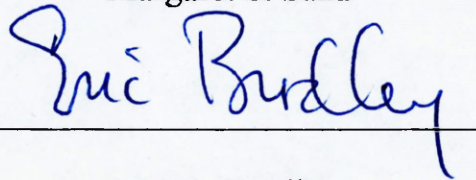


Laura Rochmis

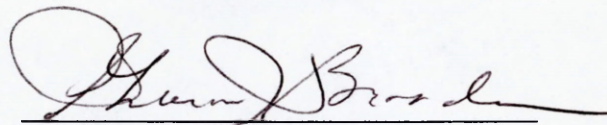
Approved, July 1995



Margaret S. Saha



Eric L. Bradley



Sharon T. Broadwater

TABLE OF CONTENTS

	Page
ACKNOWLEDGEMENTS	iv
LIST OF FIGURES	v
ABSTRACT	vii
INTRODUCTION	2
MATERIALS AND METHODS	12
RESULTS	19
DISCUSSION	25
REFERENCES	38
PLATES	43
VITA	99

ACKNOWLEDGMENTS

I would like to thank Dr. Margaret Saha for giving me the opportunity of joining her lab and for supporting my efforts in pursuing a novel direction in research. Without her enthusiasm and encouragement I would have turned back at many of the numerous roadblocks that occurred along the way. I would also like to thank the members of my committee, Dr. Eric Bradley and Dr. Sharon Broadwater, for reviewing this thesis manuscript and for providing guidance during the course of the research. A tremendous amount of technical support was provided by Jewel Thomas and Jennifer Oakes and I would like to thank them both for their unstinting generosity. The inspiration for this project came from the electron microscopy course taught by Dr. Joseph Scott and he continued to provide valuable information throughout the research. Finally, I would like to thank my parents, Ann and Paul Rochmis, for their unconditional support that has allowed me to pursue my ultimate dream.

LIST OF FIGURES

Figures	Page
1. Electron micrographs of <i>Xenopus laevis</i> , sagittal section	44
2. Transverse sections through the heart region ..	46
3. Longitudinal and sagittal sections in the heart of stage 35-37 embryos	48
4. Blood vessels overlying somite tissue	50
5. Ectodermal tissue with blood vessels	52
6. Sagittal sections showing intersomitic blood vessels	54
7. Blood vessels dorsal of the optic vesicle	56
8. Hand dissections reveal random blood vessels in the midbrain region	58
9. Serial sections from the posterior through the tail of stage 25-27 embryos	60
10. Serial sections from the posterior through the tail of stage 35-37 embryos	62
11. Correlated LM/SEM view of <i>XEGR-1</i> expression in a stage 25-27 embryo, 70 micrometers	64
12. Correlated LM/SEM view, 105 micrometers	66
13. Correlated LM/SEM view, 140 micrometers	68
14. Correlated LM/SEM view, 175 micrometers	70
15. Correlated LM/SEM view, 210 micrometers	72
16. Correlated LM/SEM view, 245 micrometers	74
17. Correlated LM/SEM view, 280 micrometers	76
18. Correlated LM/SEM view, 315 micrometers	78
19. Correlated LM/SEM view, 350 micrometers	80
20. Correlated LM/SEM view, 420 micrometers	82
21. Correlated LM/SEM view, 525 micrometers	84
22. A correlated LM/SEM view of a sagittally sectioned embryo	86

23. Correlated LM/SEM view through the posterior region of a stage 35-37 embryo, 105 micrometers	88
24. Correlated LM/SEM view, 175 micrometers	90
25. Correlated LM/SEM view, 245 micrometers	92
26. Correlated LM/SEM view, 315 micrometers	94
27. A comparison of <i>XEGR-1</i> expression in stage 25 stage 35 embryos, expression of antibody conjugated to colloidal gold	96
28. <i>XEGR-1</i> expression compared to the expression of the antibody conjugated to colloidal gold	98

ABSTRACT

Embryonic induction is a key element in the establishment of the vertebrate body plan. To understand the interactive tissue events controlling induction research has focused on the signaling pathways used during cell-cell interactions. The G-protein coupled receptor pathway was identified as an important component in adult systems, and consequently G-protein coupled receptors in developing systems are being pursued. A novel endothelial G-protein coupled receptor in *Xenopus laevis* (*XEGR-1*) was isolated and initially characterized. To expand the identification of the role this receptor plays in the processes of angiogenesis and vasculogenesis a correlated light microscopy and scanning electron microscopy study was undertaken. This involved a comparison of the domains of signal expression in a single embryo to the structural characteristics of the same embryo at the point of expression. The results of this study revealed *XEGR-1* as a marker of early inductive events in the development of the circulatory system prior to the actual formation of blood vessels. *XEGR-1* was also found to serve as a marker for structural components of the circulatory system. The development of direct labeling for the SEM will lead to more efficient and detailed methods of gene expression characterization.

A CORRELATIVE LM/SEM APPROACH TO THE MORPHOLOGICAL
CHARACTERIZATION OF GENE EXPRESSION IN *XENOPUS LAEVIS*

INTRODUCTION

Fertilization begins the process whereby a complex organism will arise from a single cell. The processes of determination, differentiation, morphogenesis, and growth that accompany this maturation are orchestrated by the genome of the organism which is contained as identical copies in each cell. The question of how a complex and heterogeneous organism is created from a single cell is explained by the concept of differential gene expression. Each cell expresses only a small portion of the entire genome, the complement of mRNA that is specific to a given cell type. The precise activation of particular genes at specific times and in specific places allows for the development of a variety of cell types and tissues.

Two factors are thought to control the differential expression of genes: (1) the presence of cytoplasmic determinants; and, (2) cell-cell interactions. Cytoplasmic determinants are maternally deposited factors present in the egg that become segregated during cleavage leading to expression or repression of specific genes in the early developmental stages of the embryo (Slack, 1991). The

mechanism governing embryonic induction is cell-cell interaction whereby one group of cells influences the fate of another group (Slack, 1993). Unlike cytoplasmic determinants inductive events continue to be fundamental to the survival of the embryo throughout development.

The inductive tissue interactions that play such an important role in embryonic development require two major components: the "inducing" tissue that gives rise to a signal and the competent "responding" tissue that receives the signal. The classic example of a series of inductive interactions is the formation and patterning of the nervous system. The primary induction of the neural ectoderm occurs, in part, through the tissue interactions between the invaginating mesoderm and the overlying ectoderm during gastrulation (Slack and Tannahill, 1992; Dixon and Kintner, 1989). In the continuing cascade of inductive interactions in the developing nervous system the neural tube responds to signals from the notochord. Cells in the neural tube adjacent to the notochord become floorplate cells (Placzek, et al., 1990; Yamada et al., 1991). These cells can, in turn, induce the formation of motor neurons from adjacent areas of the neural tube (Lumsden, 1991). The patterning of the nervous system is a complex, multi-step process that has yet to be fully elucidated, but it serves as an example of the importance of inductive interactions and cell-cell communication during development.

Inductive interactions occur in a variety of ways, but

in all cases the responding tissue must have competence to respond to the inducing tissue. Competence is often achieved through the expression of a specific receptor on the responding cell which can bind a secreted ligand or signal during the inductive interaction. The consummation of the receptor-ligand relationship leads to the activation of a second messenger pathway ending with transmission of information to the nucleus. Many different types of ligands have been isolated and studied and they continue to be the focus of much research. However, much less is known about cellular competence and the role of receptors.

Identification and classification of receptor types has led to increased knowledge about cellular interactions and may provide important tools for developmental research.

G-protein coupled receptors have been identified as a major class of proteins in adult signaling pathways, comprising roughly 80% of all known receptors (Bockaert, 1991). This class of receptors is characterized by structural similarities including seven transmembrane regions with the amino terminus in the extracellular domain and the carboxy terminus located intracellularly (Berridge, 1993; Dohlman et al., 1987). G-protein coupled receptors are involved in a variety of processes in the adult system including vision, hormone regulation, and odorant reception (Clapham, 1993). They are also implicated in a number of disease states such as cancer and hormonal imbalances (neonatal severe hyperparathyroidism) wherein there is a

mutation leading to receptor malfunction (Clapham, 1993; Pollak et al., 1993). Their importance and prevalence in the adult system has led to increased interest in the role of these receptors during development.

G-protein coupled receptors have been identified as playing a role in the earliest stages of development. For example, the G-protein-phosphoinositide pathway is responsible in part for the increase in intracellular calcium ion concentrations required for egg and sperm activation (Toratani and Yokosawa, 1995). The ubiquity of G-protein coupled receptors in the genome and the reuse of genes from development in adult organisms suggests that this is not an isolated example of G-protein coupled receptor use in development. However, despite their important role, little work has been done in embryos where signaling plays an indispensable role. For this reason an identification of G-protein coupled receptors expressed during development was attempted. The product of this work was *XEGR-1*, an endothelial receptor in *Xenopus laevis*.

XEGR-1 represents a novel cDNA cloned from a stage 42 *Xenopus laevis* cDNA library (Saha and Miles, unpublished). It is expressed in the developing embryo from neurula through swimming tadpole stages in tissues associated with angiogenesis and vasculogenesis including the developing heart, blood vessels, and angioblasts. Sequence analysis and comparison showed a 48% homology with a human gene, APJ, which is angiotensin receptor-like (O'Dowd, et al., 1993).

Further comparison to a known angiotensin receptor gene in *Xenopus* showed only 30% homology, indicating that *XEGR-1* represents a novel G-protein coupled receptor.

Two receptor subtypes have been identified as mediating the action of Angiotensin II - AT1 and AT2 (Mukoyama, et al., 1993). The AT1 receptor subtype, which is primarily expressed in adult tissues, has been well studied and characterized, showing involvement in the angiotensin II effects on cardiovascular homeostasis (Bergsma, et al., 1993; Murphy, et al., 1991). The AT2 receptor subtype has been identified mainly in young and developing organisms and has not been linked to cardiovascular function (Tsutsumi and Saavedra, 1991; Mukoyama, et al., 1993). It is not clear that *XEGR-1* belongs to either class of receptor subtypes; however, it shares many functional aspects with previously characterized AT2 receptors and is expressed during development. Further analysis of its molecular properties and its role in *Xenopus* development will clarify its identification and function.

XEGR-1 was initially characterized as a marker for angiogenesis and vasculogenesis. In vasculogenesis, blood vessels are formed *de novo* in the developing system through the aggregation of angioblasts (Pardanaud, et al., 1989; Poole and Coffin, 1989). The angioblast cells originate from mesodermal tissue and migrate to the sites of blood vessel formation. This process is differentiated from angiogenesis in that the latter involves the formation of blood vessels

from preexisting ones through budding of preformed endothelial cells (Pardanaud, et al., 1987; Folkman and Shing, 1992). Angiogenesis is thought to be responsible for the formation of intersomitic arteries and vasculature in the brain and kidneys whereas vasculogenesis accounts for the dorsal aortae, the endocardium of the primitive heart, and a proportion of the developing capillary network (Coffin et al., 1991; Coffin and Poole, 1991). Together the two processes are responsible for the development of the circulatory system, the first functional unit in the embryo. To understand how this process occurs and to differentiate between angiogenesis and vasculogenesis the developing system must be studied in greater detail.

As the organism uses the limited supply of energy from the yolk the presence of a functioning circulatory system becomes essential. The two morphogenetic processes responsible for vascular development have been best delineated by work with chick/quail chimeras (Poole & Coffin, 1989; Pardanaud, et al., 1989). During vasculogenesis angioblasts segregate from mesodermal tissue and migrate to specific sites of blood vessel formation. There they congregate into angiogenic cords which will later mature into blood vessels (Coffin, et al., 1991). The further proliferation of blood vessels from preexisting vasculature is termed angiogenesis. This process is thought to occur in most organs including the limb buds, kidney and brain (Gilbert, 1991). The functional division between

these two processes is clear; however, it is not always apparent which mechanism is responsible for certain areas of vessel formation.

The problem of differentiating between vasculogenesis and angiogenesis has been addressed using a system of antibody recognition of endothelial tissue in quail/chick chimeras. Antibodies such as QH-1 have been used to identify angioblast origin, migration, and vascular development (Pardanaud, et al., 1987; Poole & Coffin, 1989). Results of these studies indicate that all intraembryonic mesodermal tissues except the prechordal plate and the notochord contain angiogenic precursors (Noden, 1990). Areas such as the brain, spinal cord, neural crest, notochord, and prechordal mesoderm must therefore rely on the migration of angioblasts to achieve vascularization. Descriptive information on the formation of the circulatory system has been established by these experiments, but the cellular interactions involved in these processes have yet to be clarified. What has been lacking is a technique which employs an early molecular marker and detailed morphological visualization.

Many different tools have been used to analyze the formation of blood vessels. Two of the most useful were antibodies against angioblasts to localize preliminary vascular development and *in situ* hybridizations to delineate the expression pattern of genes which are markers of the developing circulatory system. To enlarge the picture

provided by these methods a morphological study combining the traditional molecular techniques of *in situ* hybridization on *Xenopus laevis* with the three dimensional view afforded by the scanning electron microscope (SEM) was pursued. *Xenopus* embryos were chosen because their large size makes them amenable subjects for both the molecular aspects of signal expression during *in situ* hybridization and the morphological manipulations required for the SEM.

Previous studies of vascular systems in adult organisms utilizing the SEM established the general surface characteristics and branching patterns of blood vessels *in vivo* allowing for description of these structures in the developing embryo (Hodde and Veltman, 1979; Phillips, et al., 1979). Identification of blood vessels in *Xenopus* was attempted using the expression pattern of *XEGR-1* as a guide to the location of specific blood vessels. In addition to the isolation of blood vessels in the developing embryo a further characterization of the gene was sought through correlative light microscopy (LM) and SEM studies.

A correlative LM/SEM method for the study of individual cells has been established allowing for both external and internal morphological characterization (Marchiondo, et al., 1994; Hayat, 1976). On the basis of these studies a method for the correlation of signal expression at the LM level with the morphological features of the same embryo at the SEM was developed for this study. Experiments concentrated on the tail region of the developing embryo at two specific

stages. *XEGR-1* is strongly and discretely expressed in the tail at both stage 25-27 and stage 35-37. The tail provides a region of study where a repetition of early development occurs spatially. As such it is an area where the growth of blood vessels can be viewed in a condensed manner with respect to the spatial aspects of development. An effort was also made to develop a method of signal identification at the SEM level.

To expand and clarify the study of the structural characteristics of the embryo at the SEM level, the standard *in situ* hybridization protocol was modified to employ an antibody conjugated to colloidal gold. The use of colloidal gold as a marker for the SEM was first proposed as a labeling method to identify cell surface receptors and relied on the increased emission of secondary electrons by the heavy metal from uncoated specimens (Horisberger et al., 1975; Horisberger et al., 1979). The ability to detect heavy metals beneath the cell surface in the backscattered electron imaging mode (BEI) of the SEM increased the usefulness of colloidal gold as a marker (DeHarven et al., 1984; Taylor et al., 1984). It can be used as an intracellular marker (at sizes < 1 nm in diameter) during *in situ* hybridization at the transmission electron microscope (TEM) level and silver enhancement allows visualization at the SEM level (Hutchison et al., 1982; Thiebaut et al., 1984). In a novel approach to characterization of gene expression after *in situ* hybridization the SEM was used to

examine embryos. In conjunction with the correlated LM/SEM study complementary cellular and molecular methods of inquiry were developed.

MATERIALS & METHODS

Animals

Sexually mature *Xenopus laevis* frogs were purchased from Xenopus I (Ann Arbor, MI). Embryos were obtained from matings induced by subcutaneous injections of human chorionic gonadotrophin (hCG) (Sigma) at concentrations of 1000 U for female frogs and 750 U for male frogs. Embryos were cultured at 14 - 16°C in 0.1 X normal amphibian media (NAM) containing 50 µg-mL⁻¹ gentamycin sulfate. All embryos used in subsequent experiments were staged according to Nieuwkoop and Faber (1967).

Whole mount in situ hybridization

Whole mount in situ hybridizations were carried out essentially as described by Harland (1991) with some modifications (Dr. Tabitha Doniach, personal communication, 1995). The gene for the novel endothelial G-protein-coupled receptor (*XEGR-1*) was isolated, sequenced, and characterized (Saha & Miles, in preparation). A probe was produced using plasmid DNA linearized with the restriction enzyme BamHI. The antisense RNA probe was transcribed with T7 RNA polymerase (Stratagene). DNase treatment and hydrolysis steps were omitted in order to synthesize the most effective

probe. Transcription reactions were performed at 37°C for 2 hours in a digoxigenin - 11 -UTP and 3H dUTP containing nucleotide mix. The 3UTP was used to determine incorporation. 0.5 uL of the completed probe was placed on two identical DE-81 filters. One filter was washed with 0.5M Na₂HPO₄ buffer to remove unincorporated radioactivity. The other filter was left unwashed. Each filter was placed in a vial containing scintillation fluid and counted on a Beckman scintillation counter. The respective counts were compared to ascertain adequate incorporation and the quantity of synthesized RNA probe.

Gelatinous coats of embryos used in the whole mount in situ procedure were removed by rinsing in a solution containing seven pellets of sodium hydroxide and 2 g of cysteine/100 mL of sterile water for 2-5 minutes, followed by three rinses in 0.1 X NAM. Embryos at different stages of development were then fixed in MEMFA (0.1 M MOPS, 2 mM EGTA, 1 mM MgSO₄, and 3.7% formaldehyde) for two hours and stored in 100% EtOH at -20°C.

After prehybridization of the embryos they were incubated overnight at 60°C with the mRNA probe in hybridization buffer (1 ug of probe per 1 mL hybridization buffer: 50% formamide, 5 X SSC, 1 mg-mL⁻¹ Torula RNA, 100 ug-mL⁻¹ heparin, 1 X Denhardt's, 0.1% Tween-20, 0.1% CHAPS, 5 mM EDTA). After removal of excess probe solution the embryos were incubated overnight at 40°C in an anti-digoxigenin antibody linked to alkaline phosphatase. Excess

antibody was removed in a series of five 1 hour washes. The chromogenic reaction was precipitated using NBT (Nitro blue tetrazolium) and BCIP (5-bromo-4-chloro-3-indolyl-phosphatase). Embryos were fixed for two hours in MEMFA and stored in 1 X PBS at 4o C for further use.

Post In Situ Hybridization Treatment

Following in situ hybridization embryos were prepared in two ways: whole mount photography and paraffin embedding and sectioning.

Stained embryos were treated with a 2:1 solution of benzyl benzoate and benzyl alcohol in order to clear the tissue prior to photography. Whole embryos were photographed on an Olympus microscope with ASA 200 film.

Embryos to be sectioned were submitted to a standard ethanol dehydration series of 50%, 70%, 80%, 90%, and 100% ethanol at five minutes per solution. They were then placed in a 50/50 ethanol/xylene solution for 10 minutes followed by 100% xylene for an additional 10 minutes. Paraffin infiltration was achieved by a 20-30 minute incubation in a 50/50 xylene/paraffin solution at 60o C followed by a three hour infiltration with 100% paraffin. Individual embryos were placed in paraffin molds in a variety of orientations and allowed to harden overnight at room temperature. Embryos were sectioned on an American Optical microtome at 10 micrometers and mounted on Meyer's adhesive treated slides on a layer of water in order to decompress the sections.

Slides were heated overnight on a heating table after which excess paraffin was removed by rapid immersion in xylene. Permanent slides were made using a 1:1 solution of permount/xylene under the coverslip.

LM/SEM Correlated Study

In order to study an individual embryo using both light microscopy (LM) and scanning electron microscopy (SEM) a variety of procedures were used. After in situ hybridization embryos were refixed in 2% glutaraldehyde in 0.1 M phosphate buffer (pH 7.2) and embedded and sectioned following the above procedures. For observation with the scanning electron microscope (SEM) the remaining portion of the embryo body in paraffin was cut out of the block and freed from paraffin with three washes in 100% xylene followed by rehydration in three changes of 100% ethanol (15 minutes each) (Watterson and Schoenwolf, 1984). The embryos were critical point dried in liquid CO₂ with a Samdri-PVT-3B critical point drier, mounted on aluminum stubs and coated with 20 nm of gold-palladium in an Anatech Hummer VII sputter coater.

Specimens were viewed on an Amray 1810 SEM at 20 kV in the standard secondary electron imaging (SEI) mode. All photography was done with a Nikon FM2 camera using TMX 402 film. For each embryo the last light microscopy section was compared to the cut surface of the embryo at the SEM level to equate stain distribution to three dimensional

morphology.

To observe the progression of signal expression through a single region of the embryo a sequential series of embryos was prepared. A series of embryos at stage 25-27 and stage 35-37 were sectioned progressively further into the tail region. The LM slides were then compared to the cut surface of the same embryo at the SEM level. To supplement the morphological analysis of these embryos similar serial sections were performed in the absence of in situ hybridization. This allowed greater structural integrity and provided a basis for morphological identification.

Morphological Studies of Embryos - SEM Preparation

Embryos were prepared for viewing on the SEM in the SEI mode by sectioning and hand dissection. Embryos for sectioning were fixed at a variety of stages in 2% glutaraldehyde in 0.1 M phosphate buffer (pH 7.2) and prepared as per post in situ hybridization embedding procedures. Embryos were sectioned to the desired area with the cut sections being discarded. The remaining embryo bodies were released from the paraffin in two changes of 100% xylene, washed three times in 100% ethanol (15 minutes each), critical point dried in liquid CO₂, mounted on aluminum stubs with double sticky tabs, and coated with 20 nm of gold-palladium.

Embryos prepared by hand dissection were first fixed in 2% glutaraldehyde in 0.1 M phosphate buffer (pH 7.2) for two

hours at room temperature. After three ten minute rinses in 0.1 M phosphate buffer hand dissections were performed. For all stages the ectoderm was removed from the dorsal side of the embryo to enable the visualization of blood vessels in the anterior dorsal region. This was done using fine glass needles under the dissecting scope. After dissection all embryos were prepared for viewing on the SEM at 20 kV as per previous procedures.

Backscattered Electron Imaging

For viewing in the backscattered electron imaging (BEI) mode on the SEM embryos were prepared following the standard in situ hybridization protocol prior to the antibody incubation. Following mRNA probe hybridization the embryos were incubated at 40 C overnight with an antidigoxygenin antibody conjugated to colloidal gold < 0.8 nm in diameter at a 1:30 dilution in standard (Maleic Acid Buffer + Boehringer Mannheim Blocking Agent + 20 % lamb serum) incubation medium (Boehringer Mannheim). Excess antibody was removed by five one hour washes in MAB. The labeling was visualized by silver enhancement reaction using a 50/50 solution of developer and enhancer solutions (Boehringer Mannheim). Embryos were incubated for one to two hours in enhancement reagents. The reaction was stopped by two successive washes in deionized distilled water (ddH₂O).

For viewing on the SEM in the BEI mode embryos were prepared using standard dehydration and mounting techniques.

After critical point drying embryos were mounted on aluminum stubs using carbon double sticky tabs edged with colloidal graphite. All specimens were coated with carbon in a Denton (DV-502) vacuum evaporator and viewed in the BEI mode at 30 kV using the A+B diode arrangement.

Controls

Controls for all SEM work involving labeling with colloidal gold were achieved either through the use of the muscle actin gene or through the omission of the correct antibody during the antibody incubation step.

Muscle actin displays a distinct and well characterized signal and was used to verify the presence of backscattered electrons as opposed to charging on embryos viewed in the BEI mode. The gene is also expressed at particular stages in development and embryos at the stage when the gene is not expressed could be used as controls.

A negative control for the *XEGR-1* probe itself was achieved through omission of the antibody during the antibody incubation step of the in situ hybridization protocol. Control embryos were subjected to the same washes, but were incubated solely in the incubation medium (MAB + 2% BMB + 20% lamb serum) overnight at 40 C.

RESULTS

The Identification of Components of the Circulatory System in *Xenopus laevis*

Paraffin embedding and sectioning of staged *Xenopus* embryos (as described in the Materials and Methods section) reveals specific structures associated with the developing circulatory system. Sagittal sections through stage 27 and stage 36 embryos show the developing heart. At stage 27 the heart anlage on the ventral side approximately opposite the hindbrain region is visible. At stage 36 the heart has developed a more complex structure (Fig. 1). Transverse sections through the anterior region at the same stages reveal the structural development of the endocardium from the ventral mesoderm and the relationship between the endocardium and the myocardium. The ventricle is located between the two structures (Fig. 2). The endocardium is enveloped by the myocardium and consists of a flattened cell layer as opposed to the the thicker myocardial structure (Fig. 3).

branching characteristics and surface texture similar to previous SEM studies (Fig. 4; see Kardon and Kessel, 1979; Phillips et al., 1979). Blood vessels were also isolated on the underside of the epidermal ectoderm overlying the somite tissue (Fig. 5) and intersomatically (Fig. 6). The sectioning of the blood vessels between the somites reveals their hollow tubular structure (Fig. 6B,C). A regular pattern of blood vessels between the somite reflects the pattern of signal expression for *XEGR-1*.

The head region of embryos provides further examples of vascularization. A blood vessel highly correlated with the expression pattern of *XEGR-1* according to its location and the stage of the embryo was isolated in the dorsal part of the head region and slightly posterior to the optic vesicle (Fig. 7). Blood vessels are also apparent after removal of the ectoderm overlying the brain (Fig. 8). They are present from the latter part of the forebrain through the hindbrain region.

Serial Sections Through the Tail of Stage 25-27 and Stage 35-37 *Xenopus* Embryos

Serial sections through the tail region of stage 25-27 and stage 35-37 embryos show the progression of structural features. In an initial section at 70 micrometers only the tailbud blastema and the epidermal ectoderm are present (Fig. 9A). Continuing sections into the tail region reveal the emergence of the somitic mesoderm flanking the neural

ectoderm and the lateral mesoderm underlying the epidermal ectoderm (Fig. 9B). The neural tube acquires its characteristic structure with the neural canal present by 140 micrometers into the tail region (Fig. 9C). The refining of these tissues continues along the anterior/posterior axis until at 245 micrometers the notochord is present as a structure distinct from the neural tube, and the lateral mesoderm is reduced to a narrow band of tissue between the yolky endoderm and the epidermal ectoderm (Fig. 9F). This reflects the development of these structures.

At stage 35-37 the *Xenopus* embryos retain many of the general tissue relationships seen in younger embryos, but many structural changes have occurred. At 105 microns the tailbud and the epidermal ectoderm are still present (Fig. 10A), but the dorsal and ventral fins are also apparent having been induced by interactions between the posterior epidermis and trunk neural crest cells (Lehman, 1977). The neural tube is discernible at 175 microns flanked by somitic mesoderm. By 245 microns the notochord can be clearly distinguished (Figs. 9B,C). More discrete patterning has emerged by 345 microns into the embryo as the myotomal structures are seen in the somitic mesoderm region at the SEM level (Fig. 9D).

Correlative LM/SEM Studies of Stage 25-27 and Stage 35-37 *Xenopus laevis* Embryos

A correlative LM/SEM view through the tail region of

stage 25-27 embryos aligns the expression of *XEGR-1* in the mesodermal tissues of the tail with its three dimensional appearance at the SEM level. The *XEGR-1* signal is diffusely expressed in the mesodermal tissue and is seen as early as 70 micrometers into the tail region. The mesodermal tissue can be distinguished from the epidermal ectoderm and the yolky endoderm at the SEM level (Figs. 11A,B). This diffuse pattern of expression correlated with the mesodermal tissues continues through 350 micrometers (Figs. 12-19). The signal becomes more refined as the tissues segregate into discrete domains. The expression continues in the lateral mesoderm even as the tissue narrows to a limited region between the epidermal ectoderm and the yolky endoderm (Fig. 14,18). The somitic mesoderm is clearly delineated at the SEM level and reflects the distinct expression in this region during *in situ* hybridization (Fig. 17,19). Signal expression begins to weaken in the mesodermal tissues at 420 micrometers (Fig. 20). The pattern of expression acquires a punctate appearance at 525 micrometers in the lateral mesodermal areas. No clear structures can be seen at the SEM that correlate with this altered signal pattern (Fig. 21).

In stage 35-37 embryos the expression of *XEGR-1* occurs in a more limited area in the tail region. Longitudinal sectioning shows the extent of the signal expression along the anterior/posterior axis as well as laterally across the tissues of the tail (Fig. 22). Transverse sections through the tail region clarify the extent of signal expression

along the anterior/posterior axis. At 105 micrometers the gene is strongly expressed in the somitic mesodermal tissues at the LM level (Fig. 23A). At the SEM level the neural tube can be distinguished, but there is no apparent differentiation between the mesoderm and endoderm (Fig. 23B). The gene is still expressed weakly at 175 micrometers, but by 245 micrometers there is no longer a distinct signal at the LM level (Fig. 25A). The SEM view at 245 micrometers does show a clear separation between the neural tube and notochord, and the somitic tissue can be distinguished (Fig. 25B, 26B).

Whole Mount Expression of *XEGR-1*

Whole mount *in situ* hybridizations performed on *Xenopus* embryos were used as a guide for correlative LM/SEM studies. Hybridizations were performed on stage 25-27 and stage 35-37 embryos. At stage 25-27 a strong signal is visible in the tail region. A more diffuse signal appears in the area of the developing tail and the head, but no distinct structural staining is apparent (Fig. 27A). At stage 35-37 there is a conspicuous decrease in the signal in the tail region. The gene is still strongly expressed in the head and can now be clearly seen in the heart, the vessels flanking the notochord, and intersomatically (Fig. 27A).

Whole embryos incubated with the colloidal gold conjugated antibody show gene expression after silver enhancement. *XEGR-1* expression can be seen in the tail, the

heart, between the somites and in the head of stage 35-37 embryos (Fig. 27B). In comparative views of silver stained embryos to normally stained embryos the signal is clearer and more easily visualized in embryos after the normal color reaction in both stage 25-27 and stage 35-37 embryos; however, the similar patterns of expression confirm that there is no lack of expression in the antibody coupled to colloidal gold (Fig. 28).

DISCUSSION

The elucidation of the processes involved in development of the circulatory system has important implications not only for our understanding of developmental biology, but also for our understanding of such events as tumorigenesis. Understanding angiogenesis and vasculogenesis is the first step in achieving a broader grasp of the development of the circulatory system. To study these processes a genetic marker, *XEGR-1*, was employed because its involvement in the development of the circulatory system has been established. An understanding of the complex developmental events involved requires not only an effective marker, but also the ability to visualize distinct morphological characteristics and processes in which the gene is involved.

Angiogenesis and vasculogenesis create a system of blood vessels and related structures that form through unique patterning events during development. The vascular system is not limited to the symmetrical characteristics of many developing structures such as the neural tube and somites. There are paired or symmetrical blood vessels such as the dorsal aortae and intersomitic blood vessels, but there is also a vast amount of unique vascularization occurring in the developing embryo. To follow this growth

and establish the timing of involvement of *XEGR-1* a novel experimental approach was taken.

Preliminary studies of *XEGR-1* showed the gene to be expressed from early stages throughout the development of the organism until the swimming tadpole stage, but it remained unclear whether it was a marker for early vasculogenesis in addition to a marker for the developed circulatory system. To explore this question embryos were examined at both the LM and SEM levels to determine if gene expression was associated with detectable morphological differences. LM sections taken from an embryo were compared with SEM views of the morphology of the same embryo. This correlation of signal and morphology enhanced the characterization of gene expression. Additional signal correlation was attempted at the SEM level using the BEI capacity of the microscope, but was only partially successful. Combined with structural studies of serially sectioned embryos the role of *XEGR-1* in vasculogenesis and angiogenesis was clarified.

Identification of Morphological Characteristics Using the Scanning Electron Microscope

Morphological analysis of *Xenopus laevis* embryos using several different preparations reveals a three dimensional view of external and internal characteristics

not readily visible at the light microscope level. Preparation of a variety of stages of embryos by paraffin embedding, sectioning and subsequent retrieval of the embryo body from the paraffin gave a clear view of internal structures. In the anterior region the development of the heart through a variety of stages was followed. The initial appearance of the heart anlage was noted at stage 25-27. The complex structures of the endocardium, pericardial cavity and myocardium had developed by stage 35-37. The endocardium could be easily distinguished from the myocardium by tissue surface characteristics. The relatively large structures of the heart associated with angiogenesis were readily discernible. Individual blood vessels were also identified with the earliest blood vessels isolated at stage 22 in this study.

Blood vessels associated with the somite tissue were isolated. They appeared both as overlying vasculature and in the intersomitic junctions. The intersomitic blood vessels are thought to arise through angiogenesis and as such their labeling indicates that *XEGR-1* is expressed in angiogenic tissues.

Blood vessel isolation in other regions of gene expression was more difficult. In transversely sectioned embryos blood vessels along the anterior/posterior axis became indistinguishable from the surrounding tissue. To

visualize blood vessels in the head region the outer ectodermal layer was removed to reveal the underlying brain. The vasculature on the surface of the brain was isolated in this manner. There does not appear to be a pattern in this region; however, the method of embryo preparation may have disrupted the organization of the underlying network.

The identification of blood vessels in specific regions of *XEGR-1* expression supported the characterization of this gene as an endothelial G-protein coupled receptor involved in angiogenesis and vasculogenesis. An expanded characterization of *XEGR-1* and additional molecular work in this area will support G-protein coupled receptor involvement in these processes (unpublished, Saha, et al.).

Whole Mount Expression of *XEGR-1*

The expression pattern of *XEGR-1* at specific stages was examined to establish a basis for further aspects of the study. Whole mount in situ hybridization performed on tailbud (stage 25-27) and hatching (stage 35-37) embryos showed distinct patterns of expression in such areas as the heart, the intersomitic regions, the tailbud region and the head. This first step in the characterization of *XEGR-1* served as a basis for morphological examination using the scanning electron microscope.

***XEGR-1* and its Involvement in Angiogenesis and Vasculogenesis**

Sequence analysis suggested that the gene was a member of the G-protein coupled receptor family (Miles, Master's Thesis). The expression pattern of the gene suggested that it might be involved in the cell-cell interactions influencing the development of the circulatory system. Other receptor systems such as the tyrosine kinase receptor *flk-1* and its high affinity ligand VEGF (vascular endothelial growth factor) have been identified as regulators of vasculogenesis and angiogenesis (Millauer, et al., 1993). In addition to the tyrosine kinase superfamily the G-protein coupled receptor family also seems to play a role in the two processes. The use of a human vascular endothelial cell line as a model for angiogenesis gave indirect evidence of G-protein receptor involvement after the application of pertussis toxin (an inhibitor of G-protein mediated signaling) inhibited cell motility (Bauer, et al., 1992). Additional studies gave more indirect evidence through the identification of angiotensin II as a mediator of angiogenesis, possibly through a G-protein coupled receptor (Stirling, et al., 1990). A third study indicated the presence of an induced G-protein coupled receptor after application of the tumor promoter phorbol

12-myristate 13-acetate (Hla and Maciag, 1990). The addition of *XEGR-1* to this list supports the involvement of G-protein coupled receptors in the development of the circulatory system. With the molecular role of *XEGR-1* narrowed down a more detailed characterization must rely on a variety of methods such as non traditional microscopy techniques and alternative methods of sequence visualization.

Correlated Light Microscopic and Scanning Electron Microscopic Studies of *XEGR-1* Expression

The correlative LM/SEM study of gene expression provided valuable information concerning the morphological characteristics of the embryo with respect areas of gene expression. During the study it became apparent very early that the *in situ* hybridization procedure greatly affected the cellular structure in the embryo. At the SEM level tissues appeared compressed and gaps were visible in between the cells of the ectoderm. In order to avoid overlooking any loss of internal morphological characteristics initial sequences of serially sectioned embryos at stage 25-27 and stage 35-37 were prepared at the SEM level.

Stage 25-27 embryos showed a structural progression through the tailbud region. Epidermal ectoderm could be readily distinguished from all underlying tissues in all

embryos. Lateral plate mesoderm and somitic mesoderm were both visible and showed clear separation from the yolky endoderm. In the dorsal region the neural tube was first discernible. Its appearance was followed closely by that of the notochord. In some embryos there was not a clear division between the two structures showing the tendency of some tissue to collapse or merge with adjacent structures. This problem generally occurred only in tissues flanked by air spaces and is most likely a by product of the critical point drying process.

The internal structures of the stage 35-37 embryos were very similar in composition to those of the stage 25-27 embryos, but they did display some differences. The neural tube and the notochord appeared earlier in the sectioning and more consistently retained separate domains. This difference may be due to the more advanced development of the structures at this stage in which they show more autonomy and a greater bulk in relation to the surrounding tissues. The lateral plate mesoderm occupies a narrower region and the somitic mesoderm extends farther into the tailbud region. The older stage embryos display a more refined pattern but retain the same tissue relationships as the younger stage.

Traditional correlative studies have employed the light microscope and the transmission electron microscope using sequential thick and thin sections of the same

specimen. A novel single application method of correlation was developed to use the LM in conjunction with the SEM (Marchiando, et al., 1994). This study inspired an attempt to correlate signal expression after *in situ* hybridization in LM sections with the cut surface of the same embryo at the SEM level. Previous use of paraffin embedded and sectioned embryos with the SEM indicated that this attempt at correlation was feasible despite the lack of previous work in this field (Watterson and Schoenwolf, 1984).

Serial sections through the tail region of *Xenopus* embryos after *in situ* hybridization provided the LM sections for the study. *XEGR-1* is expressed in the lateral plate mesoderm and the somitic mesoderm in both stage 25-27 embryos and stage 35-37 embryos in this region. Correlation with the SEM view of the tail region showed no apparent vasculature in these regions. At stage 25-27 the tissue in the most posterior region does not appear to be differentiated into vascular structures and morphological texts do not show the presence of any blood vessels in this region at this stage (Lehman, 1977). In the most anterior regions of the embryo the stain becomes less diffuse and displays a punctate pattern of expression. This may reflect the presence of blood vessels such as the dorsal aorta or internal carotid artery. The correlative study at this stage indicates

that *XEGR-1* is expressed in tissues prior to blood vessel formation and therefore might serve as an early marker for vasculogenesis or angiogenesis.

Stage 35-37 embryos showed the same pattern of expression at the LM level with signal apparent in mesodermal tissues; however, the signal is expressed in a more limited region of the tail. Despite the presence of blood vessels such as the dorsal aorta and the posterior cardinal vein well into the tail region there is no strong signal outside of the mesodermal tissues. No identification of these structures was made in embryos at the SEM level. Correlation at this stage indicates a decrease in the expanse of signal expression and a similar decrease at the SEM level of undifferentiated tissue areas.

Correlative studies provide an invaluable view of the morphological development and relationships of tissues that express a particular gene. The limitations of this method lie in the lack of definition of particular tissue types and the alterations in embryo structure that can occur during preparation of specimens for the SEM. A direct method for signal expression at the SEM level would alleviate some of these problems.

Backscattered Electron Imaging and Gene Expression

The development of the backscattered electron detector for the SEM increased the potential uses of this form of microscopy. In the BEI mode the SEM can detect the presence of different atomic weight elements through their increased emission of backscattered electrons (de Harven, et al., 1984; Holgate, et al., 1983). We attempted to take advantage of this technique by labeling *XEGR-1* with an antibody conjugated to colloidal gold. The size of the gold particles was < 0.8 nm which allowed their entry into the cells. In order to visualize this signal at the SEM level the signal was increased using the colloidal gold silver staining (CGSS) method which precipitates silver onto the gold particles (Holgate, et al., 1983).

The embryos were first examined at the LM level as whole mounts. The silver stain could be visualized in the tail, head, somite and heart regions at various stages in the same pattern as the standard color reaction. The novel use of this antibody in a whole mount embryo, as opposed to embryo sections, was successful. Unfortunately the success at the SEM level has not been established due to the difficulty in obtaining a sufficient coating of carbon (a low atomic weight element) on the embryo to provide conductivity. Should coating be successful this technique promises to be a powerful tool for examination

of gene expression at the SEM level, bridging the gap between light microscopy and transmission electron microscopy.

Future Directions

The experiments performed in this paper represent a preliminary attempt to correlate gene expression at two levels of microscopy. The continuation of this work should initially concentrate on a similar methodology applied to areas of gene expression in the embryo outside of the tailbud region. A variety of regions, stages and sectioning orientations would elucidate the role of *XEGR-1* with respect to angiogenesis and vasculogenesis by providing support for the idea of gene expression in undifferentiated and differentiated tissues.

A second area of continued study lies in the attempt to study signal expression directly at the SEM level. To support the findings that the antibody conjugated to colloidal gold is actually labeling intracellularly (at the sites of mRNA expression) post *in situ* hybridization tissue can be examined at the TEM level where visualization of the gold probe is possible. Confirmation of the presence of the gold probe would support the work done in the BEI mode.

To continue the attempts to visualize gene expression at the SEM level carbon coating of the

specimen must be achieved. It is possible that the inability to adequately coat with carbon is due to the condition of the embryo which may be actively repelling the carbon due to a charge on the embryo. This difficulty should be approached at the mechanical level by an examination of the chemicals used during *in situ* hybridization and by an assessment of the available coating techniques. When an adequate coating is achieved to allow visualization in the BEI mode this method may prove a powerful tool for characterization of a variety of genes.

At the molecular level there are many approaches that should be pursued. The identification of the ligand for *XEGR-1* would provide valuable clues to its role in vasculogenesis and angiogenesis. Potential ligands might first be pursued in substances such as angiogenin which have been shown to bind to endothelial receptors (Hu, et al., 1991). *XEGR-1* expression should also be compared to the expression of sequentially and functionally similar receptors in *Xenopus*.

Finally, the correlation studies should be continued with additional genes in *Xenopus* embryos. Genes expressed in a more restricted area, such as *XENK* in the forebrain, would provide a more limited study area. Comparison with additional genes involved in the dorsal/ventral patterning of the forebrain would refine the

identification of morphological differences between cells. The expansion of LM/SEM correlated studies to include genes expressed across various regions of the embryo and in a variety of tissue types will increase our understanding and appreciation of this method of morphological characterization as a tool in developmental biology.

REFERENCES

- Bauer, J., Margolis, M., Schreiner, C., Edgell, C., Azizkhan, J., Lazarowski, E. and Juliano, R.L. (1992) In Vitro Model of Angiogenesis Using a Human Endothelial-Derived Permanent Cell Line: Contributions of Induced Gene Expression, G-Proteins, and Integrins. *Journal of Cellular Physiology*, 153: 437-449.
- Bergsma, D., Ellis, C., Nuthulaganti, P., Nambi, P., Scaife, K., Kumar, C. and Aiyar, N. (1993) Isolation and Expression of a Novel Angiotensin II Receptor from *Xenopus laevis* Heart. *Molecular Pharmacology*, 44: 277-284.
- Berridge, Michael J. (1993) Inositol Triphosphate and Calcium Signaling. *Nature*, 361: 315-325.
- Bockaert, J. (1991) G proteins and G-protein coupled Receptors: Structure, Function and Interactions. *Current Opinion in Neurobiology*, 1: 32-42.
- Clapham, David E. (1993) Mutations in G Protein-Linked Receptors: Novel Insights on Disease. *Cell*, 75: 1237-1239.
- Coffin, J., Harrison, J., Schwartz, S. and Heimark, R. (1991) Angioblast Differentiation and Morphogenesis of the Vascular Endothelium in the Mouse Embryo. *Developmental Biology*, 148: 51-63.
- Coffin, Douglas J. and Poole, Thomas J. (1991) Endothelial Cell Origin and Migration in Embryonic Heart and Cranial Blood Vessel Development. *The Anatomical Record*, 231: 383-395.
- de Harven, E., Leung, R., and Christensen, H. (1984) A Novel Approach for Scanning Electron Microscopy of Colloidal Gold-labelled Cell Surfaces. *The Journal of Cell Biology*, 99: 53-57.
- Dixon, Jane E. and Kintner, Chris R. (1989) Cellular Contacts Required for Neural Induction in *Xenopus* embryos: Evidence for Two Signals. *Development*, 106: 749-757.

Dohlman, H., Caron, M. and Lefkowitz, R. (1987) A Family of Receptors Coupled to Guanine Nucleotide Regulatory Proteins. *Biochemistry*, vol. 26, no. 10: 2657-2664.

Folkman, Judah and Shing, Yuen. (1992) Angiogenesis. *The Journal of Biological Chemistry*, vol. 267, no. 16, 10931-10934.

Gilbert, S. (1991) Developmental Biology, 3d. ed. Sinauer Associates, Inc.; Sunderland, Massachusetts.

Harland, R. (1991) In situ hybridization: an improved method for Xenopus embryos. *Methods in Cell Biology*, 36: 685-695.

Hayat, M.A. (ed.) (1976) Principles and Techniques of Scanning Electron Microscopy, Vol. 5. Von Nostrand Reinhold Co.; New York.

Hla, Timothy and Maciag, Thomas. (1980) An Abundant Transcript Induced in Differentiating Human Endothelial Cells Encodes a Polypeptide with Structural Similarities to G-protein-coupled Receptors. *The Journal of Biological Chemistry*, vol. 265, no. 16: 9308-9313.

Hodde, K.C. and Veltman, W.A.M. (1979) The Vascularization of the Pineal Gland (Epiphysis Cerebri) of the Rat. *Scanning Electron Microscopy*, 3: 369-374.

Holgate, C., Jackson, P., Cowen, P. and Bird, C. (1983) Immunogold- Silver Staining: New Method of Immunostaining with Enhanced Sensitivity. *The Journal of Histochemistry and Cytochemistry*, vol. 31, no. 7: 938-944.

Horisberger, Marc. (1979) Evaluation of Colloidal Gold as a Cytochemical Marker for Transmission and Scanning Electron Microscopy. *Biol. Cellulaire*, 36: 253-258.

Horisberger, M., Rosset, J. and Bauer, H. (1975) Colloidal Gold Granules as Markers for Cell Surface Receptors in the Scanning Electron Microscope. *Experientia*, 31: 1147-1149.

Hu, G., Chang, S., Riordan, J. and Vallee, B. (1991) An Angiogenin-Binding Protein From Endothelial Cells. *Proc Nat'l Acad Sci USA*, 88: 2227-2231.

Hutchison, N., Langer-Safer, P., Ward, D. and Hamkalo, B. (1982) In Situ Hybridization at the Electron Microscope Level: Hybrid Detection by Autoradiography and Colloidal Gold. *J Cell Biology*, 95: 609-618.

Kardon, R.H. and Kessel, R.G. SEM Studies on Vascular Casts of the Rat Ovary. *Scanning Electron Microscopy*, III: 743-749.

Lehman, H.E. (1977) Chordate Development, Hunter Publishing Company, University of North Carolina - Chapel Hill.

Lumsden, Andrew. (1991) Motorizing the Spinal Cord. *Cell*, 64: 471-473.

Marchiando, A.A. & Conder, G.A. (1994) A Correlative LM/SEM Method. *USA Microscopy and Analysis*, 11:11.

Millauer, B., Wizigmann-Voos, S., Schnurch, H., Marinez, M., Moller, N., Risau, W. and Ullrich, A. (1993) High Affinity VEGF Binding and Developmental Expression Suggest Flk-1 as a Major Regulator of Vasculogenesis and Angiogenesis. *Cell*, 72: 835-846.

Mukoyama, M., Nakajima, M., Horiuchi, M., Sasamura, H., Pratt, R. and Dzau, R. (1993) Expression Cloning of Type 2 Angiotensin II Receptor Reveals a Unique Class of Seven-transmembrane Receptors. *The Journal of Biological Chemistry*, vol. 268, no. 33, 24539-24542.

Murphy, T.J., Alexander, R., Griendling, K., Runge, M. and Bernstein, K. (1991) Isolation of a cDNA Encoding the Vascular Type-1 Angiotensin II Receptor. *Nature*, 351: 233-236.

Nieuwkoop, P.D. and Faber, J. (1967) Normal table of *Xenopus laevis* (Daudin). Amsterdam: North Holland Publishing Co.

Noden, D.M. (1989) Embryonic origins and assembly of blood vessels. *American Review of Respiratory Disease*, 140:1097-1103.

O'Dowd, D., Heiber, M., Chan, A., Heng, H., Tsui, L., Kennedy, J., Shi, X., Petronis, A., George, S., and Nguyen, T. (1993) A Human Gene That Shows Identity With the Gene Encoding the Angiotensin Receptor is Located on Chromosome 11. *Gene*, 136 (102): 355-360.

Pardanaud, L., Yassine, F. and Dieterlen-Lievre, F. (1989) Relationship Between Vasculogenesis, Angiogenesis and Haemopoiesis During Avian Ontogeny. *Development*, 105, 473-485.

Pardanaud, L., Altmann, C., Kitos, P., Dieterlen-Lievre, F. and Buck, . (1987) Vasculogenesis in the Early Quail Blastodisc as Studied with a Monoclonal Antibody Recognizing Endothelial Cells. *Development*, 100, 339-349.

Phillips, S., Rosenberg, A., Meir-Levi, D. and Pappas, . (1979) Visualization of the Coronary Microvascular Bed by Light and Scanning Electron Microscopy and X-Ray in the Mammalian Heart. *Scanning Electron Microscopy*, 3: 735-740.

Placzek, M., Tessier-Lavigne, M., Yamada, T., Jessell, T. and Dodd, J. (1990) Mesodermal Control of Neural Cell Identity: Floor Plate Induction by the Notochord. *Science*, 250: 985-988.

Pollak, M., Brown, E., Chou, Y., Hebert, S., Marx, S., Steinmann, B., Levi, T., Seidman, C. and Seidman, J. (1993) Mutations in the Human Ca^{2+} -Sensing Receptor Gene Cause Familial Hypocalciuric Hypercalcemia and Neonatal Severe Hyperparathyroidism. *Cell*, 75: 1297-1303.

Poole, T. and Coffin, D. (1989) Vasculogenesis and Angiogenesis; Two Distinct Morphogenetic Mechanisms Establish Embryonic Vascular Pattern. *The Journal of Experimental Zoology*, 251:224-231.

Slack, J.M.W. (1991) From Egg to Embryo. Cambridge University Press; New York.

Slack, J.M.W. (1993) Embryonic Induction. *Mechanisms of Development*, 41:91-107.

Slack, J.M.W. and Tannahill, D. (1992) Mechanisms of Anteroposterior Axis Specification in Vertebrates: Lessons from the Amphibians. *Development*, 114: 285-302.

Stirling, D., Magness, R., Stone, R., Waterman, M. and Simpson, E. (1990) Angiotensin II Inhibits Luteinizing Hormone-stimulated Cholesterol Side Chain Cleavage Expression and Stimulates Basic Fibroblast Growth Factor Expression in Bovine Luteal Cells in Primary Culture. *The Journal of Biological Chemistry*, vol. 265, no. 1, 5-8.

Taylor, J.S.H., Fawcett, J.W. & Hirst, L. (1984) The Use of Backscattered Electrons to Examine Selectively Stained Nerve Fibers in the Scanning Electron Microscope. *Stain Technology*, 59, no. 6, 335-341.

Thiebaut, F., Rigaut, J., Feren, K., and Reith, A. (1984) The Application of the Nucleolar Organizer Region Silver Staining (AgNOR) to Backscattered Electron Imaging (BEI). *Biology of the Cell*, 52: 103-108.

Toratani, Satoshi and Yokosawa, Hideyoshi. (1995) Evidence for the Involvement of the Rho GTP-binding Protein in Egg Activation of the Ascidian *Halocynthia roretzi*. *Development Growth and Differentiation*, 37: 31-37.

Tsutsumi, Keisuke and Saavedra, Juan M. (1991) Differential Development of Angiotensin II Receptor Subtypes in the Rat Brain. *Endocrinology*, vol. 128, no. 1, 630-632.

Watterson, Ray L. and Schoenwolf, Gary C. (1984) Laboratory Studies of Chick, Pig, and Frog Embryos: Guide and Atlas of Vertebrate Embryology. Burgess Publishing Company: Minnesota.

Yamada, T., Placzek, M., Tanaka, H., Dodd, J., and Jessell, T.M. (1991) Control of Cell Pattern in the Developing Nervous System: Polarizing Activity of the Floor Plate and Notochord. *Cell*, 64: 635-647.

Figure 1. Comparative views of sagittally sectioned *Xenopus laevis* embryos at stages 27 and 36. Sections through the heart show the increasing complexity of the structure. (A) A stage 27 embryo showing the heart rudiments, indicated by arrowheads, 49X. (B) A later stage 36 embryo showing the more complex structures of the heart (H), 41X.

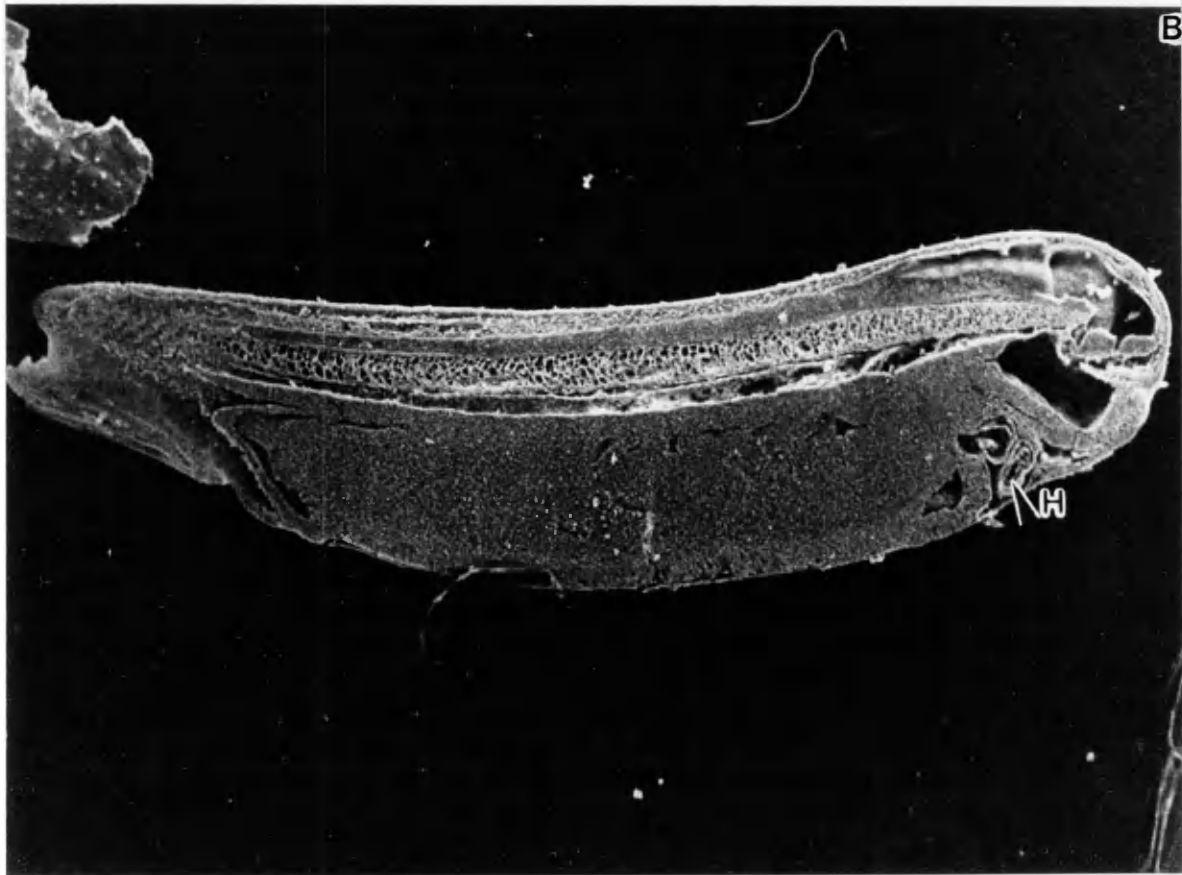
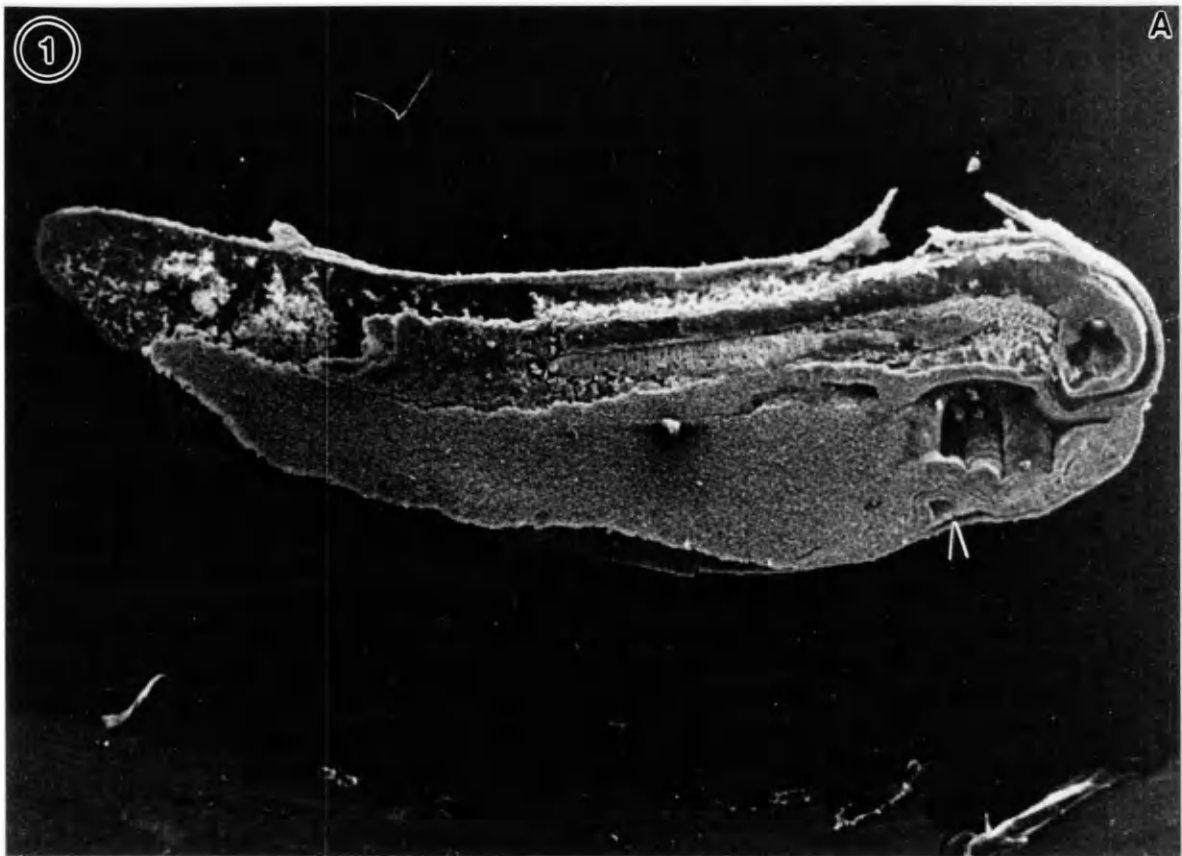


Figure 2. A comparative view of transversely sectioned *Xenopus laevis* embryos at stages 27 and 36. (A) An anterior view of a transversely sectioned stage 27 embryo orients the presumptive heart (H) with respect to the foregut (F), notochord (NC) and neural tube (NT), (97X). (B) A higher magnification of (A), (732X). (C) A stage 36 embryo, transverse section, (88X). (D) A higher magnification of (C) shows the more complex heart structures including the endocardium (E), pericardial cavity (PC), ventricle (V) and the myocardium (M), (654X).

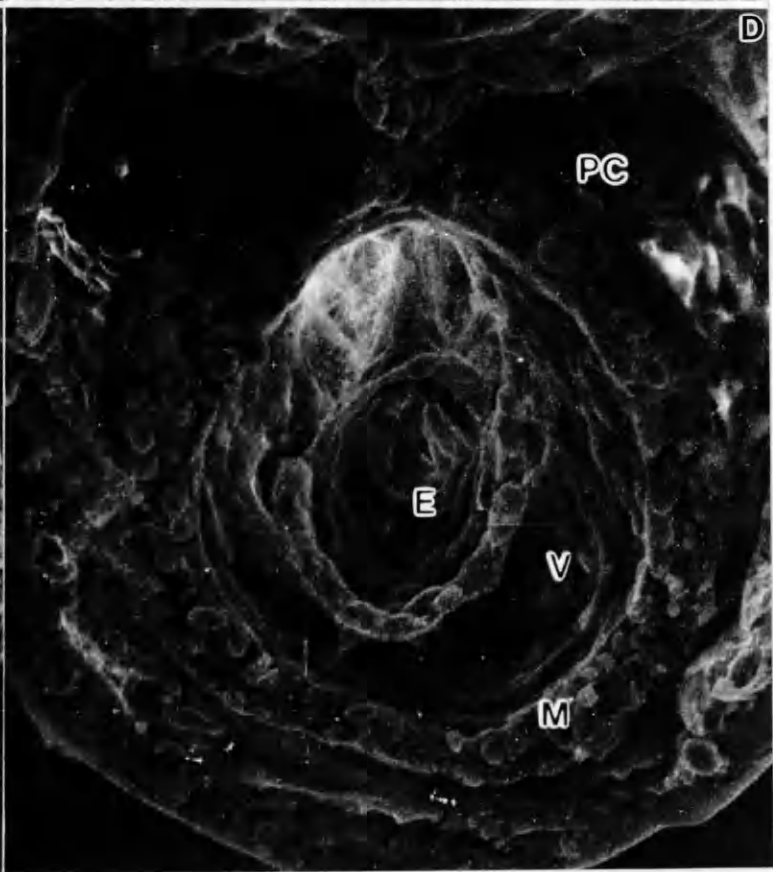
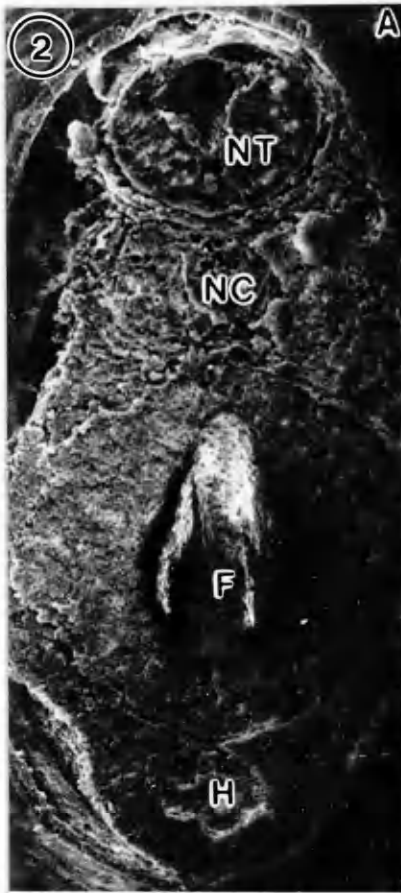


Figure 3. Longitudinally and sagittally sectioned stage 36 *Xenopus laevis* embryos reveal the structural composition of the heart. (A) A longitudinal section from the ventral side shows the myocardium (MC) and endocardium (E), 123X (left) and 344X (right). (B) A sagittal section shows the endocardium (E), pericardial cavity (PC), and the myocardium (MC), 450X.

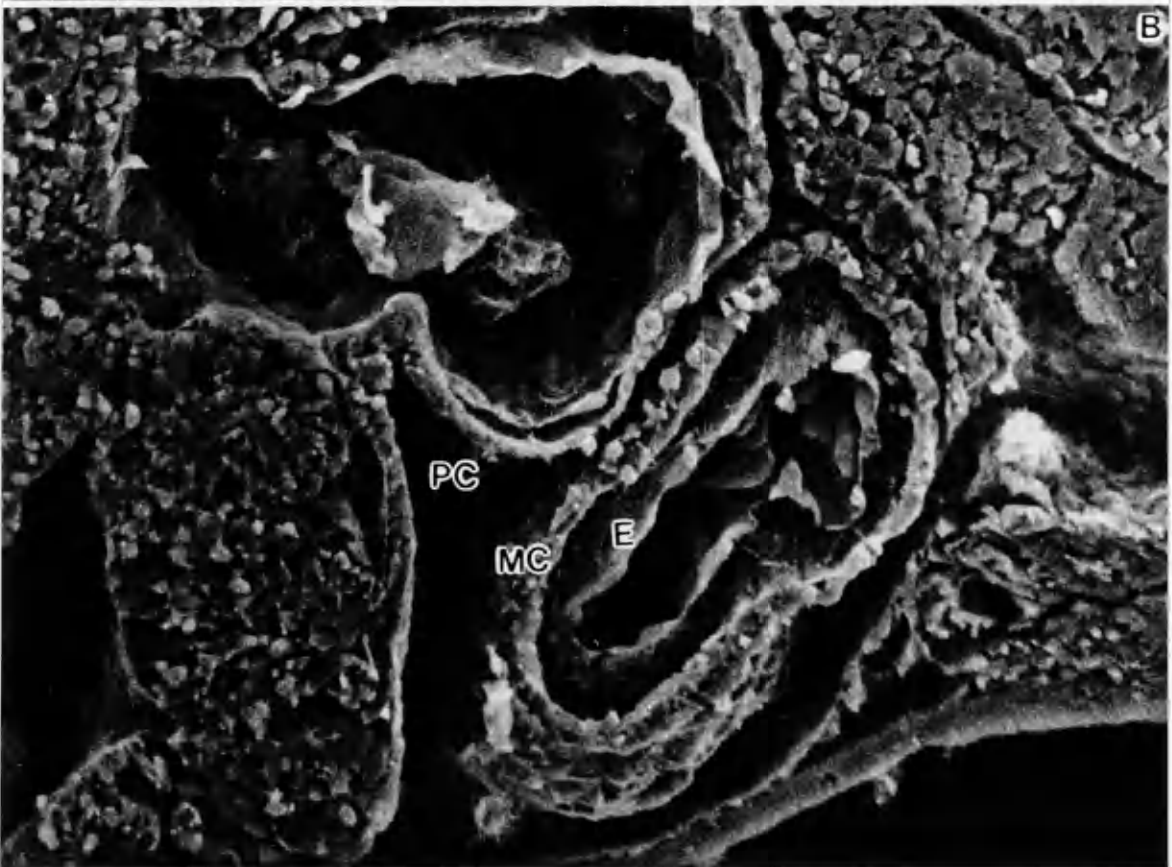
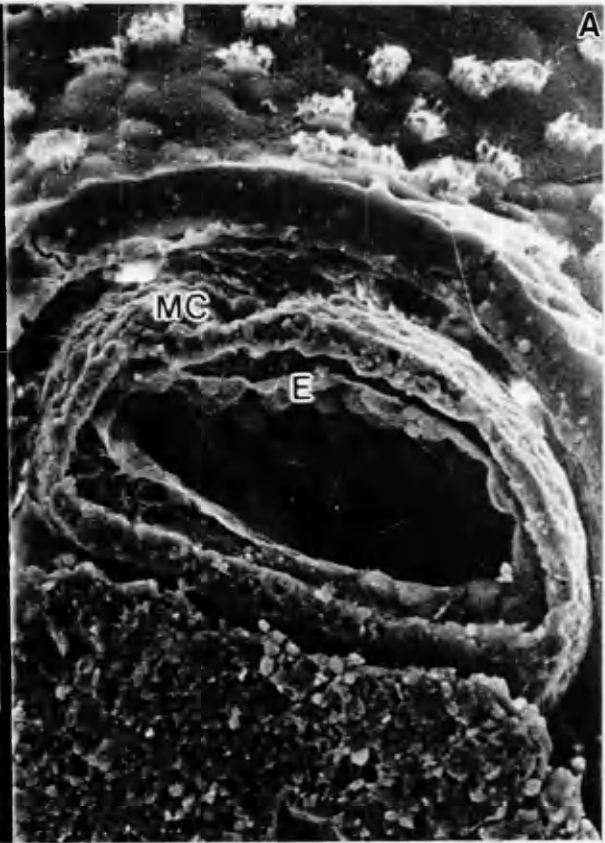
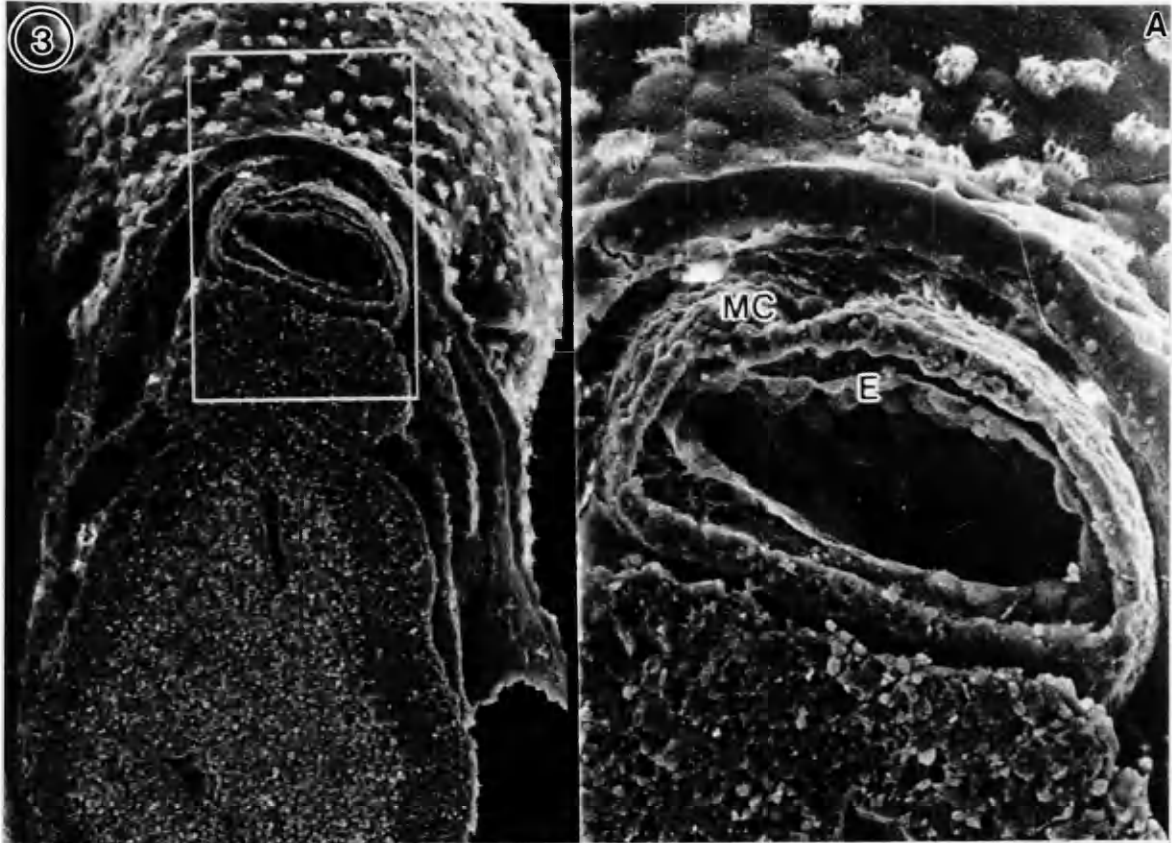


Figure 4. Paraffin embedded and sectioned stage 40 *Xenopus laevis* embryos. All scanning electron micrographs represent sagittally sectioned embryos and show the somitic tissue flanking the neural tube. Note the presence of overlying blood vessels (BV) on the muscle fibers (M). (D) Arrowheads indicate an area of blood vessel branching, 2336X.

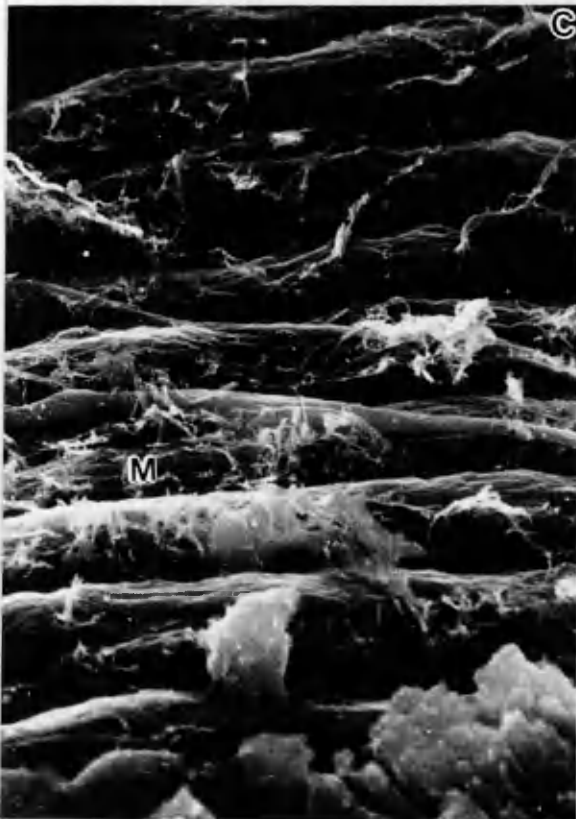
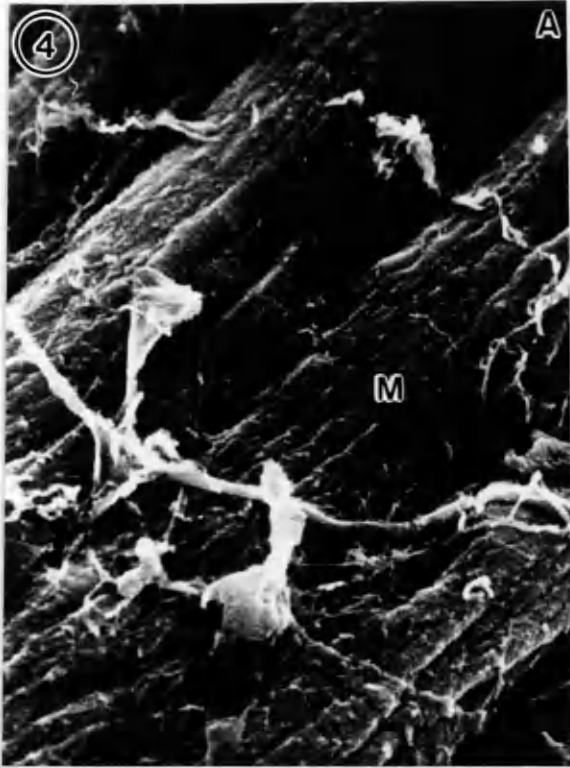


Figure 5. Paraffin embedded and sectioned stage 35 *Xenopus laevis* embryos. The ectoderm has fallen away from the somitic tissue to reveal the highly vascularized underside. (A) Low magnification view of the ectodermal tissue showing the somitic involutions with arrowheads indicating the blood vessels, 444X. (B) High magnification view of the vascularization of the ectoderm showing a network of blood vessels (arrowheads), 1438X. (C) Higher magnification of individual blood vessels indicated by arrows, 2027X.

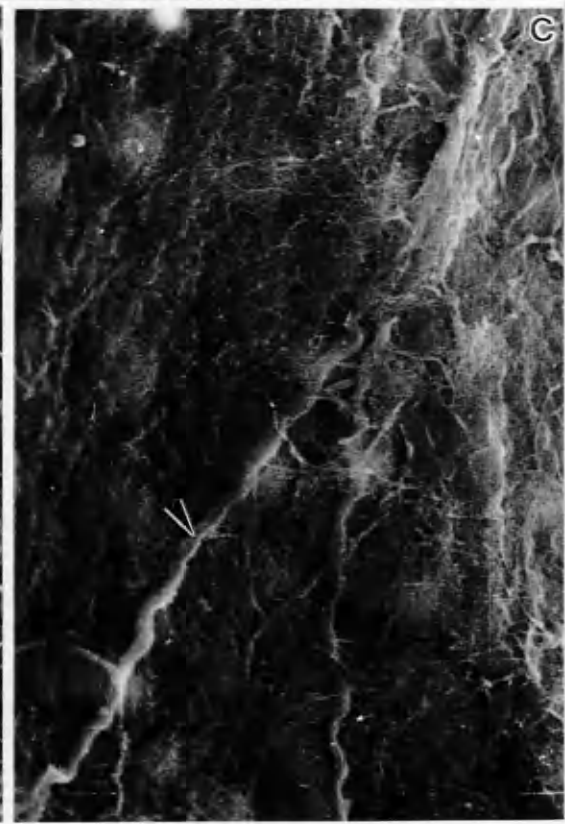
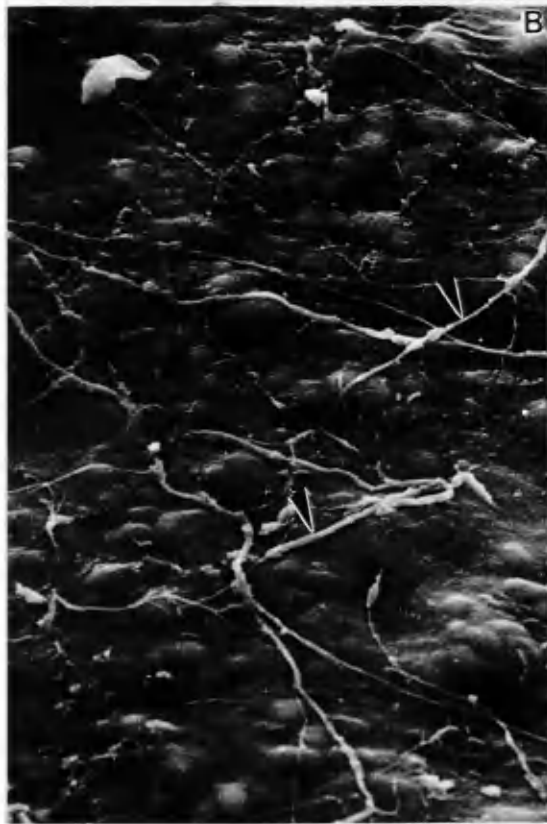
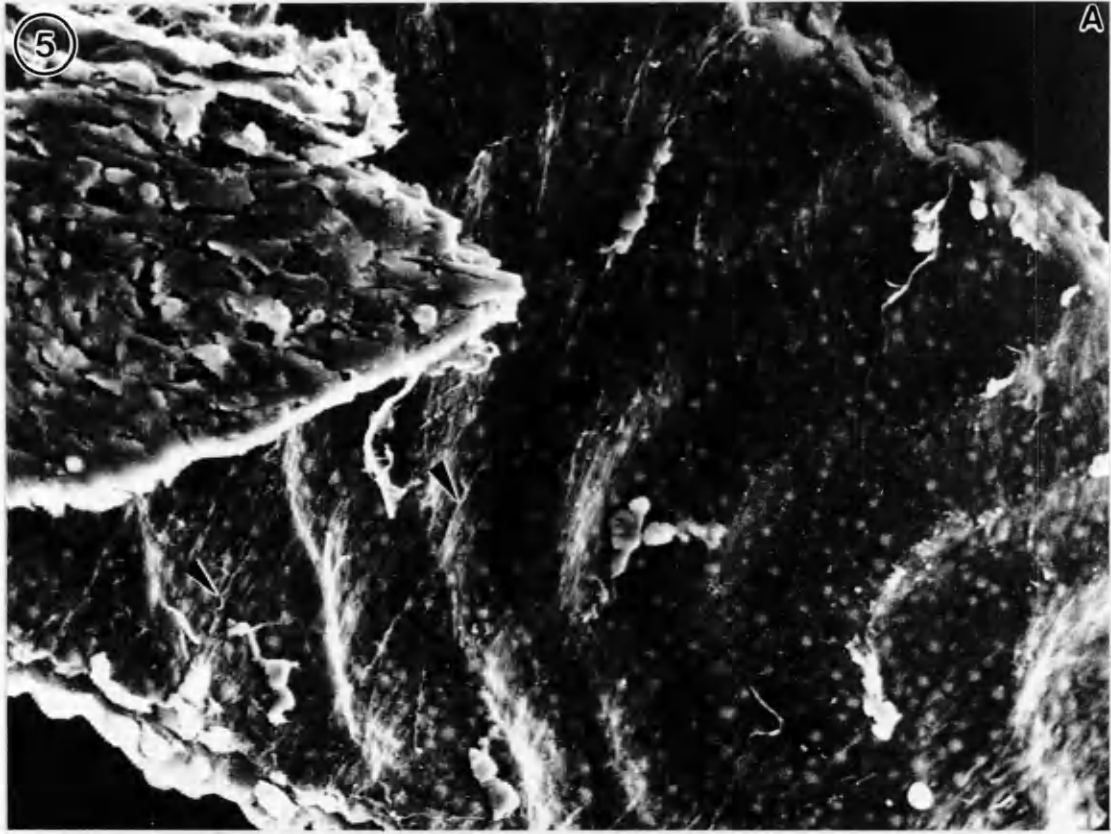


Figure 6. Paraffin embedded and sectioned stage 35 *Xenopus laevis* embryos. Sagittally sectioned embryos reveal somite tissue and blood vessels. In situ hybridization results indicate signal in the intersomitic areas. (A) Stage 35 embryo showing sagittal view of somites (S) with the presence of intersomitic blood vessels (BV, arrowheads) 534X. (B) and (C) Higher magnification views of intersomitic blood vessels (arrowheads), 4035X (left) and 2043X (right).

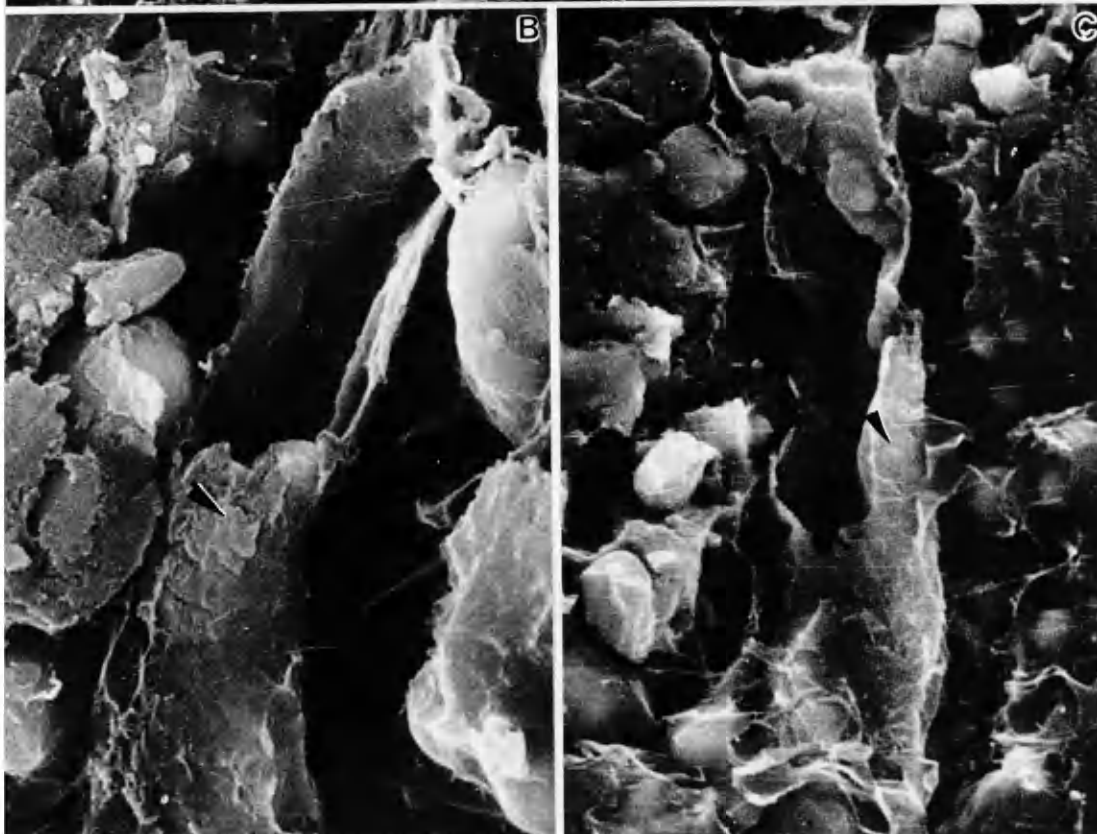


Figure 7. A sagittally sectioned stage 36 *Xenopus laevis* embryo. Whole mount in situ hybridization indicates a discrete signal in the dorsal anterior area of the head at this stage. (A) Sagittally sectioned embryo reveals the developing brain (B) and the presence of a blood vessel (arrowheads) located above the optic vesicle (OV), 113X. (B) High magnification view of the emerging blood vessel, 4127X.



Figure 8. Hand dissections of stage 36 *Xenopus laevis* embryos. The overlying ectoderm in the dorsal anterior region was removed to reveal nervous system structures and associated blood vessels. (A) Blood vessels (arrowheads) over the hindbrain area, 4248X. (B) Blood vessels (arrowheads) overlying the midbrain region, 1055X (left), 7713X (right).

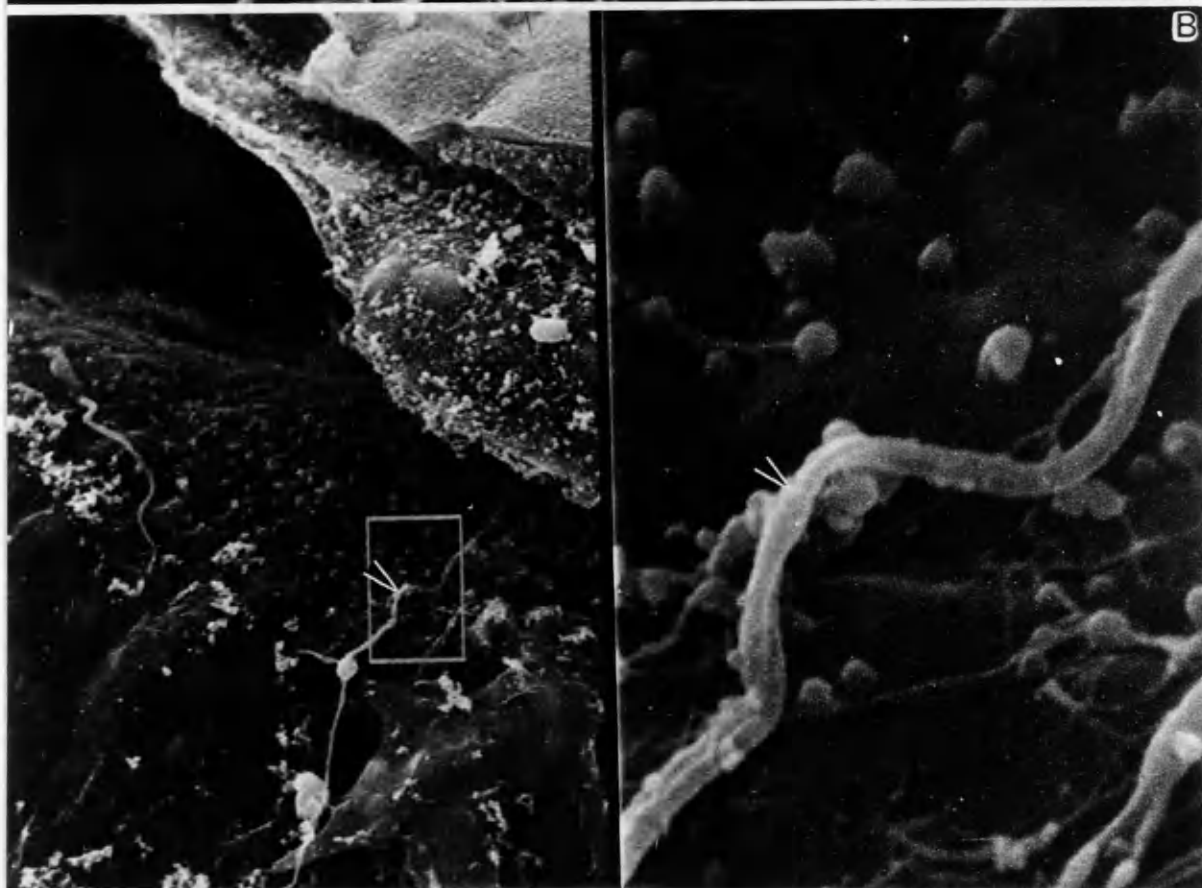
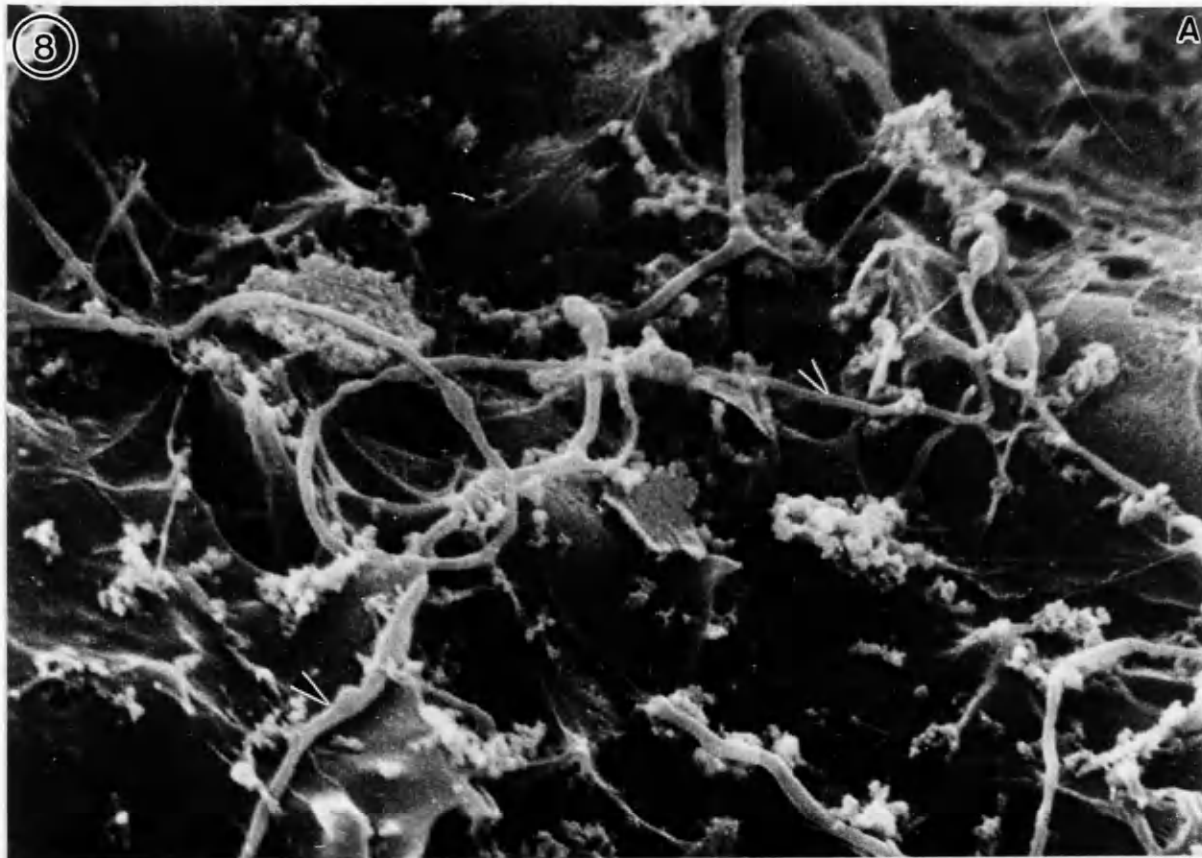


Figure 9. Serial transverse sections through the tail of stage 25-27 embryos. (A) 70 micrometers into the tail shows the epidermal ectoderm (**EE**) and the tailbud blastema (**TB**). (B) At 105 micrometers the emergence of the lateral mesoderm (**LM**) is evident flanking the neural ectoderm (**NE**). (C) At 140 micrometers the neural tube (**NT**) and the hindgut (**HG**) are visible. (D) At 175 micrometers the somitic mesoderm (**SM**) is distinct from the neural tube. (E) At 210 micrometers into the tail the lateral mesoderm (**LM**) flanks the hindgut region. (F) At 245 micrometers the notochord (**NC**) underlies the neural tube. Also visible are the lateral mesoderm (**LM**) and the yolky endoderm (**YE**).

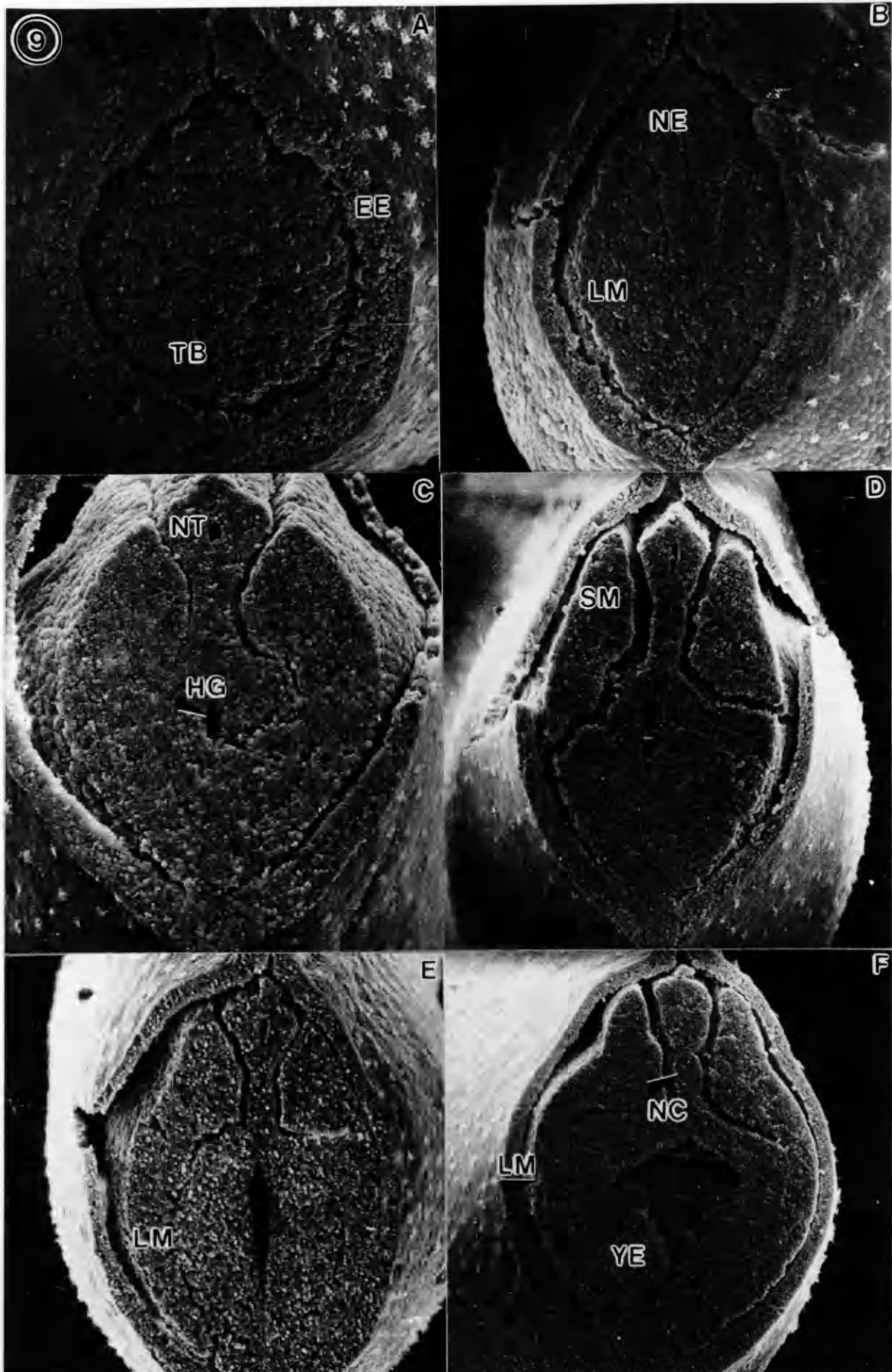


Figure 10. Serial transverse sections through the tail of stage 35-37 embryos. (A) 105 micrometers into the tail shows the epidermal ectoderm (EE) and the tailbud (TB). The dorsal fin (DF) and ventral fin (VF) are also visible. (B) At 175 micrometers the neural tube (NT) is visible. (C) At 245 micrometers the notochord (NC) underlies the neural tube. (D) 315 micrometers into the tail shows the somitic mesoderm (SM) flanking the neural tube.

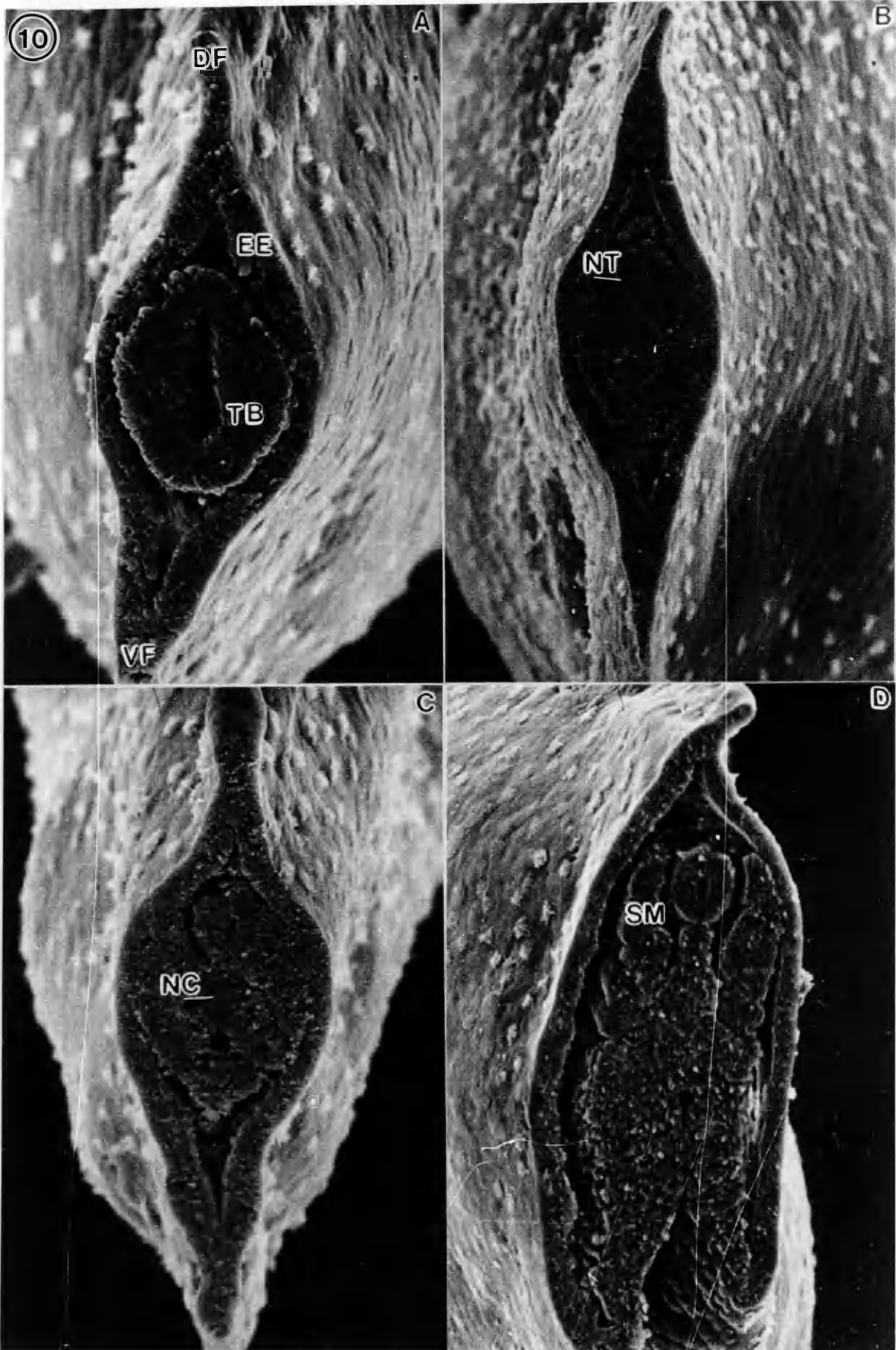
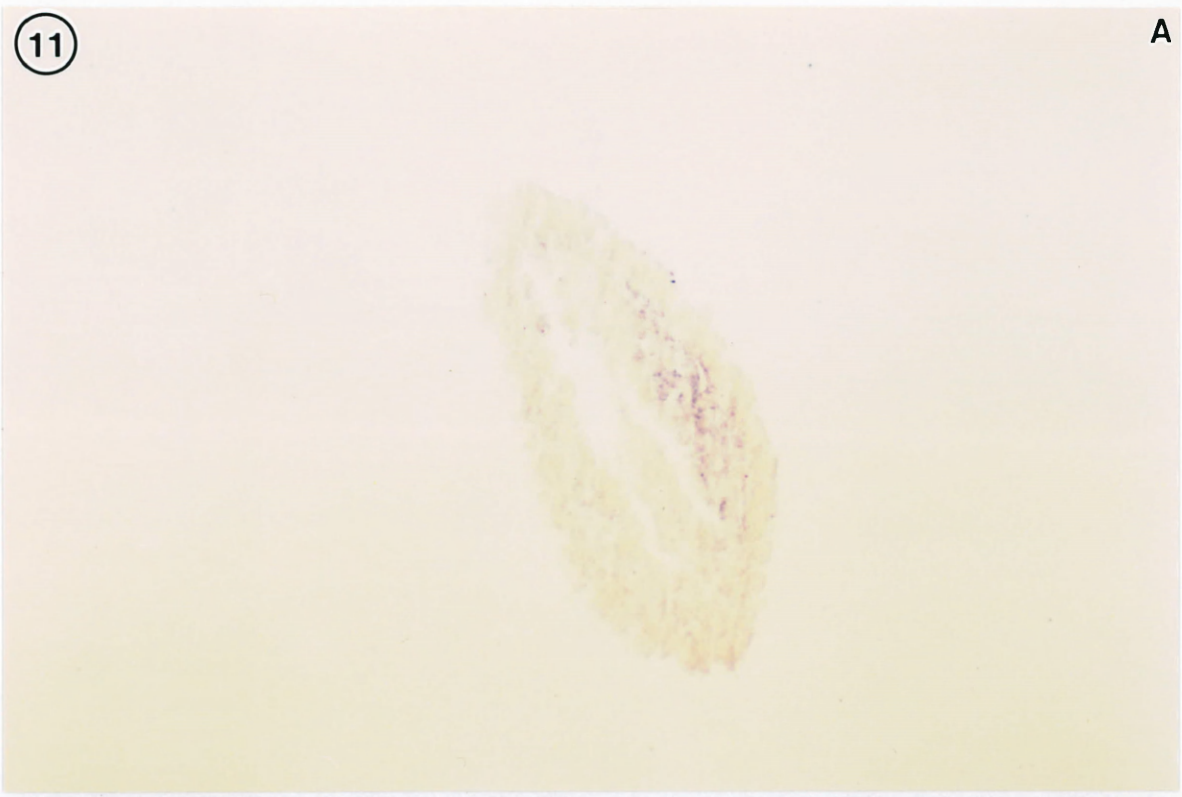


Figure 11. A light microscope (LM) and scanning electron microscope (SEM) correlated view of a transversely sectioned stage 25-27 embryo. The embryo has been sectioned 70 micrometers into the tail region. (A) The expression of *XEGR-1* in the tail region shows gene expression in the lateral mesoderm in a diffuse pattern, 100X (B) The SEM view of the same embryo. The epidermal ectoderm (EE), mesoderm (M) and yolky endoderm (YE) can be differentiated, 197X.

11

A



B

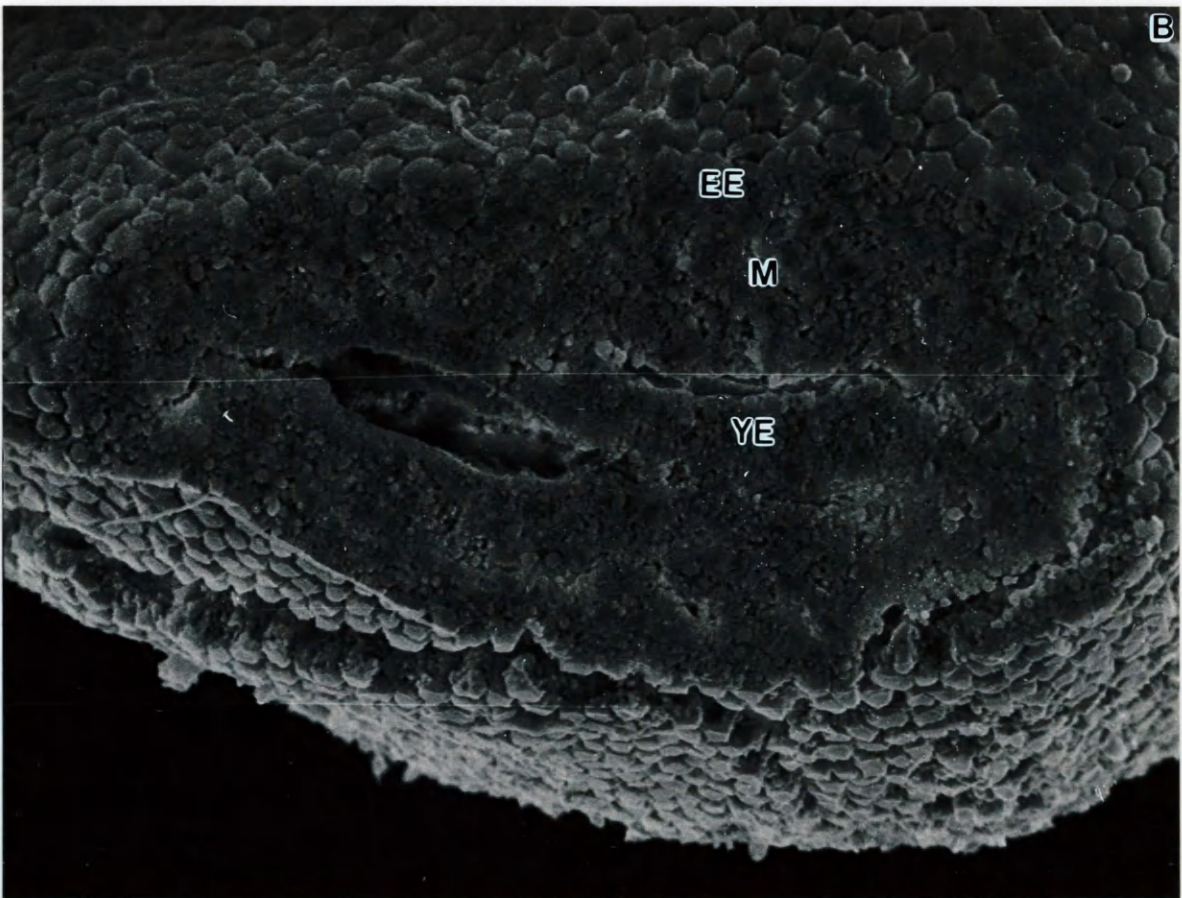


Figure 12. An LM/SEM correlation of a stage 25-27 embryo sectioned to 105 micrometers. (A) *XEGR-1* expression appears in the lateral mesoderm (LM) in a diffuse pattern, but is absent in the ectodermal and endodermal tissues (arrowheads), 100X. (B) An SEM view of the surface of the same embryo, 154X.

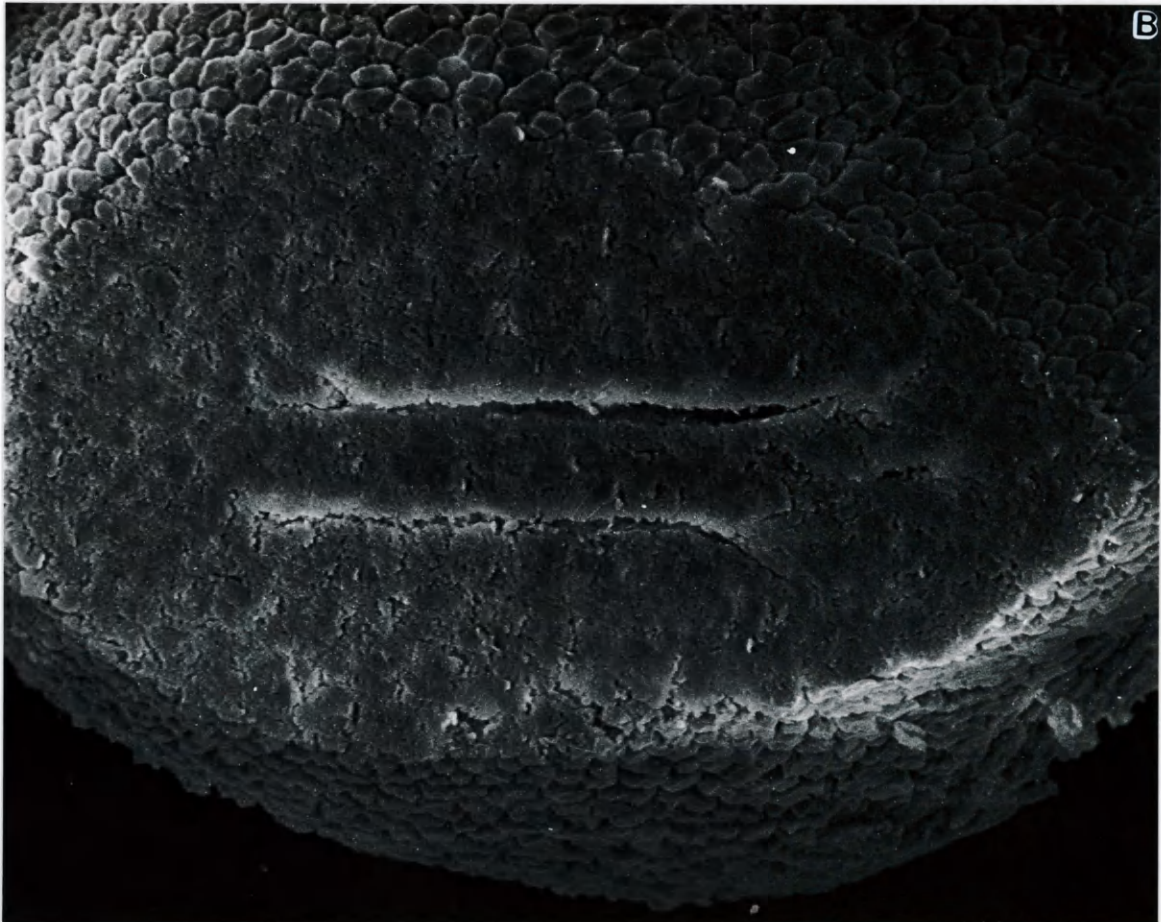
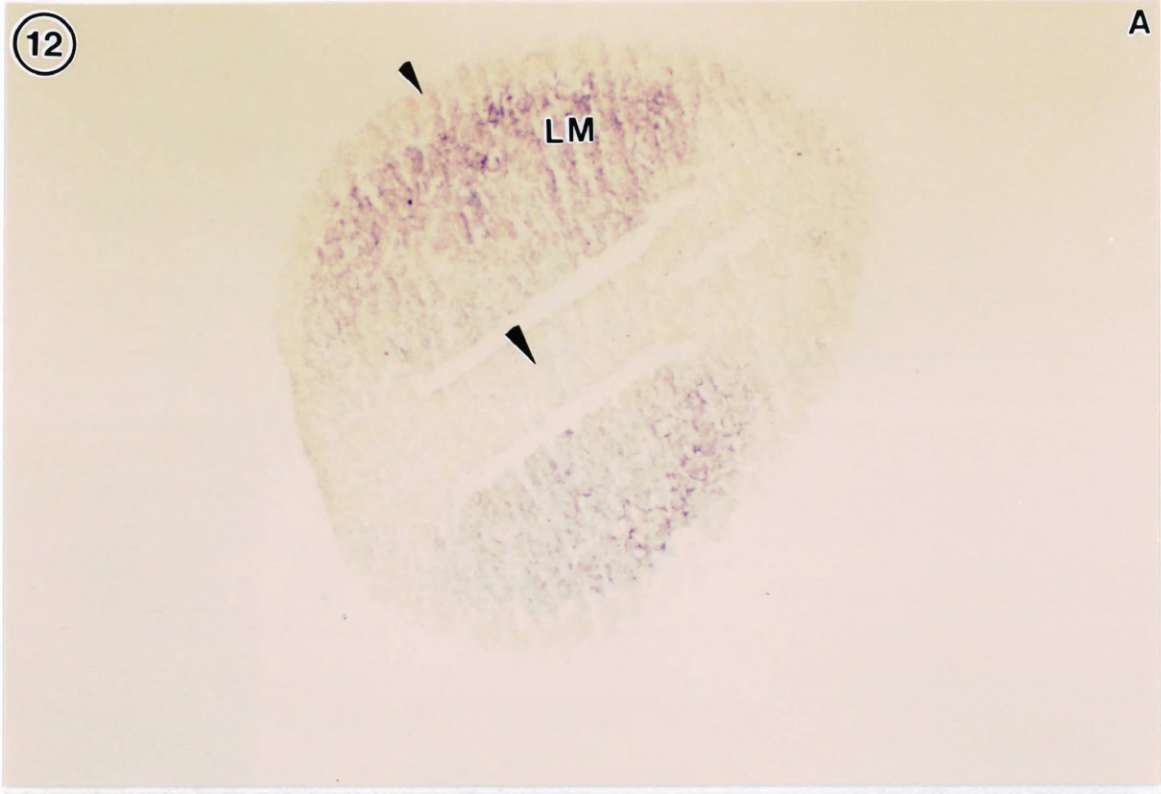


Figure 13. A stage 25-27 embryo transversely sectioned to 140 micrometers. (A) *XEGR-1* expression is absent in the emerging neural tube, the endoderm, and the epidermal ectoderm, 100X. (B) An SEM micrograph of the same embryo. The neural tube (NT) is distinct from the mesodermal tissues (arrowheads), 125X.

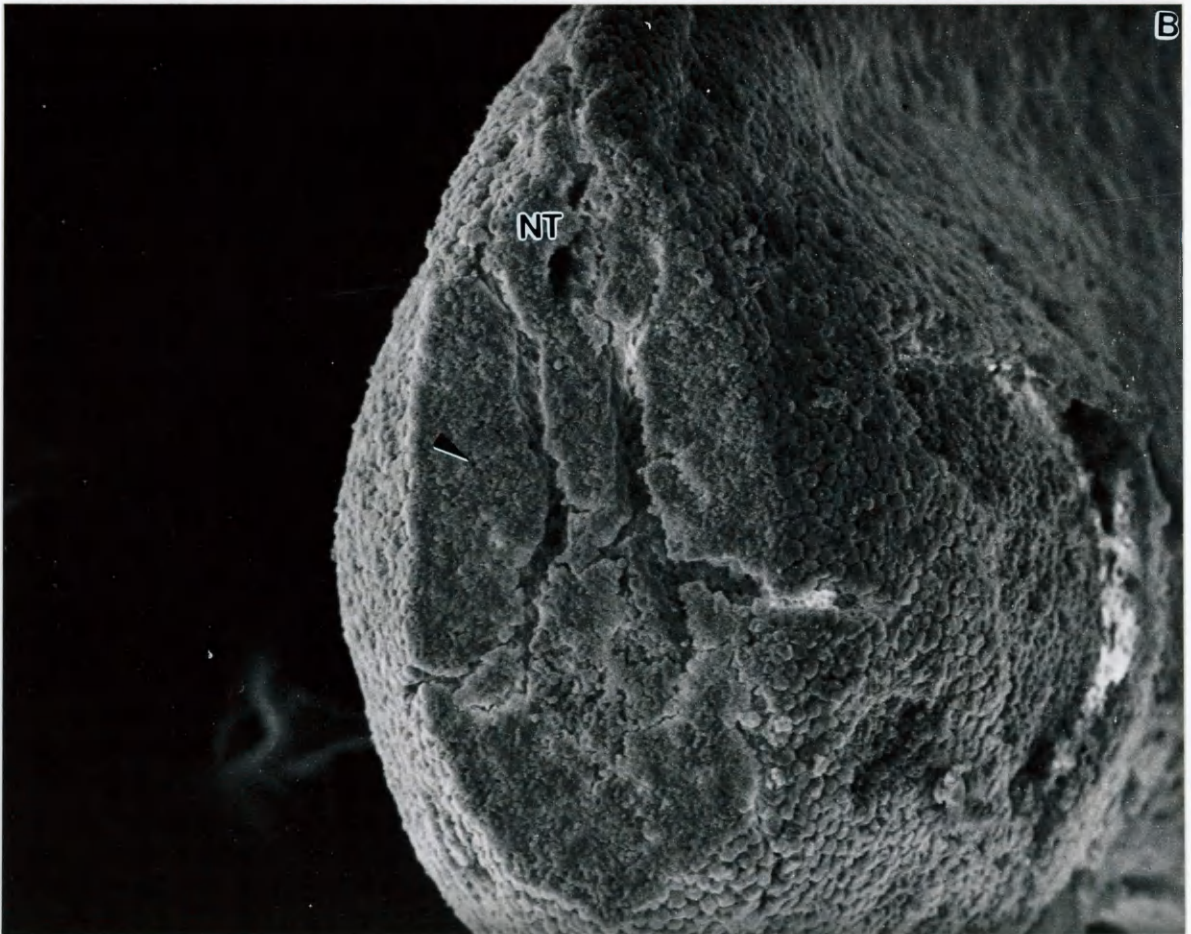
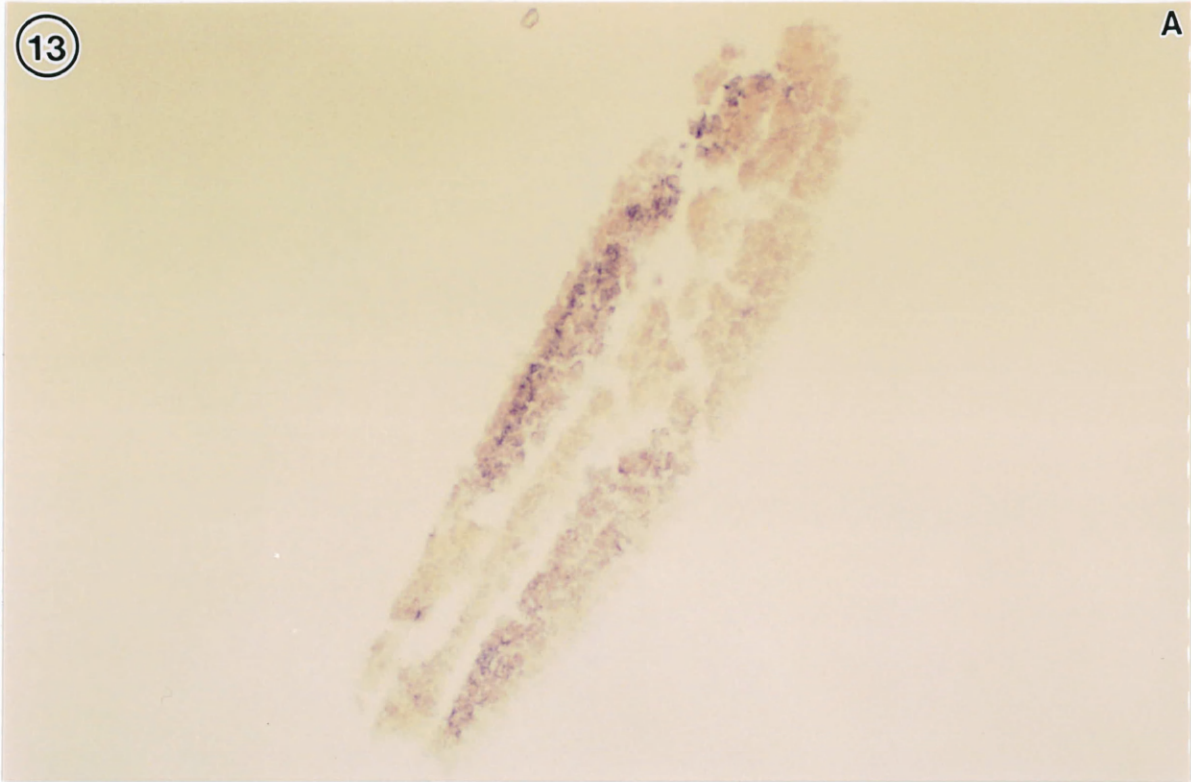
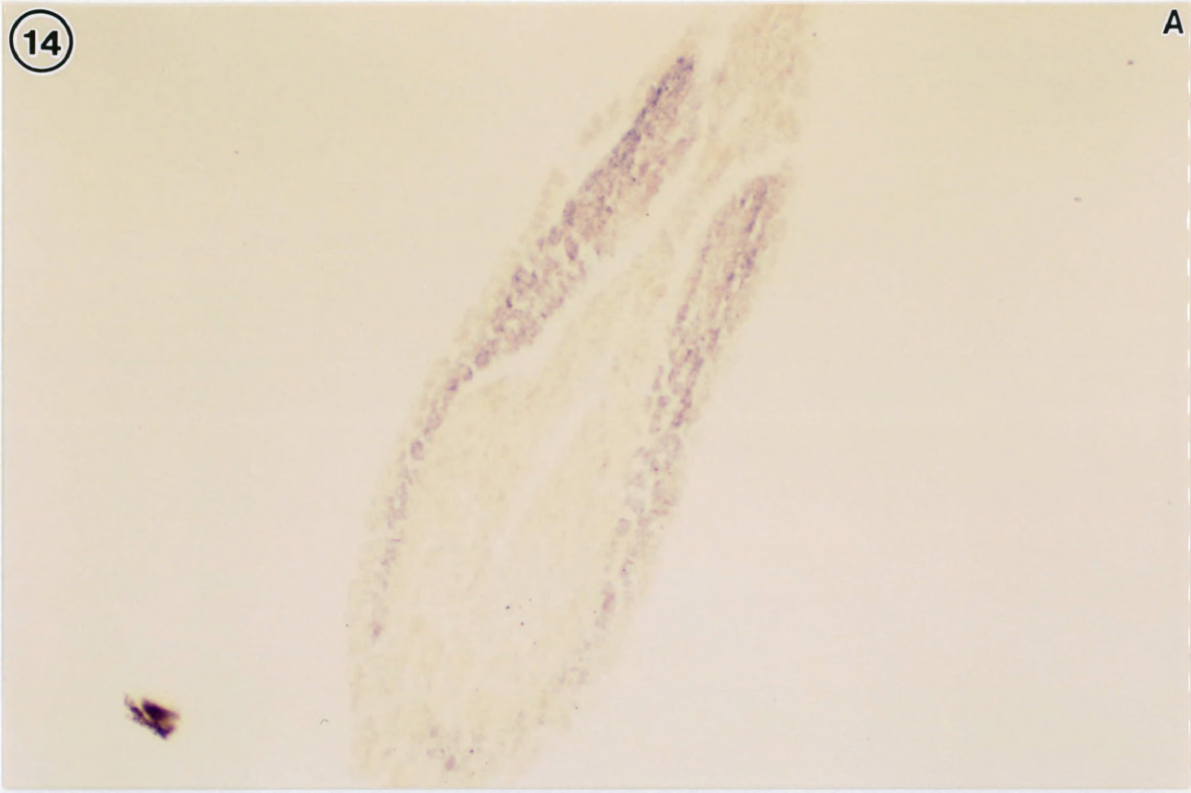


Figure 14. A transverse section at 175 micrometers through the tail region of a stage 25-27 embryo. (A) The somitic and lateral mesoderm shows distinct signal in the LM view of the embryo, 100X. (B) The tissue areas are distinct in the SEM view, but there are no apparent structural differences correlated with the presence of the diffuse signal, 130X.

14

A



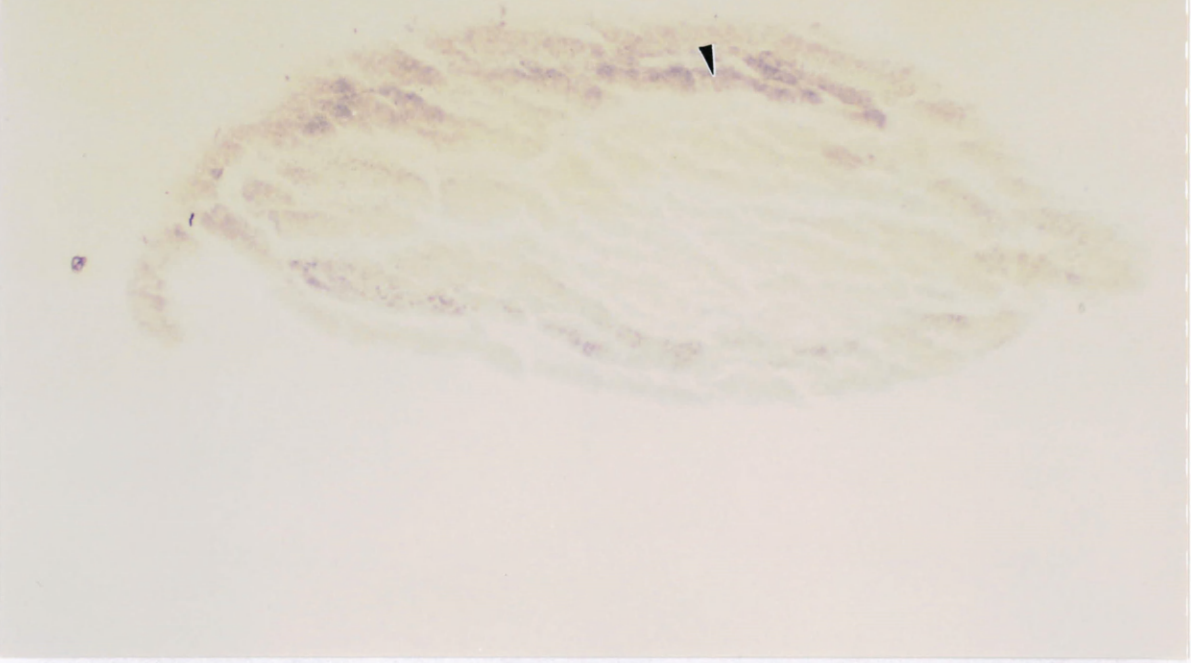
B



Figure 15. A stage 25-27 embryo transversely sectioned through the tail region. (A) The signal is concentrated in the lateral edges of the mesodermal tissue (arrowhead), 100X. (B) At 210 micrometers the neural tube(NT) and notochord(NC) are visible, 117X.

15

A



B

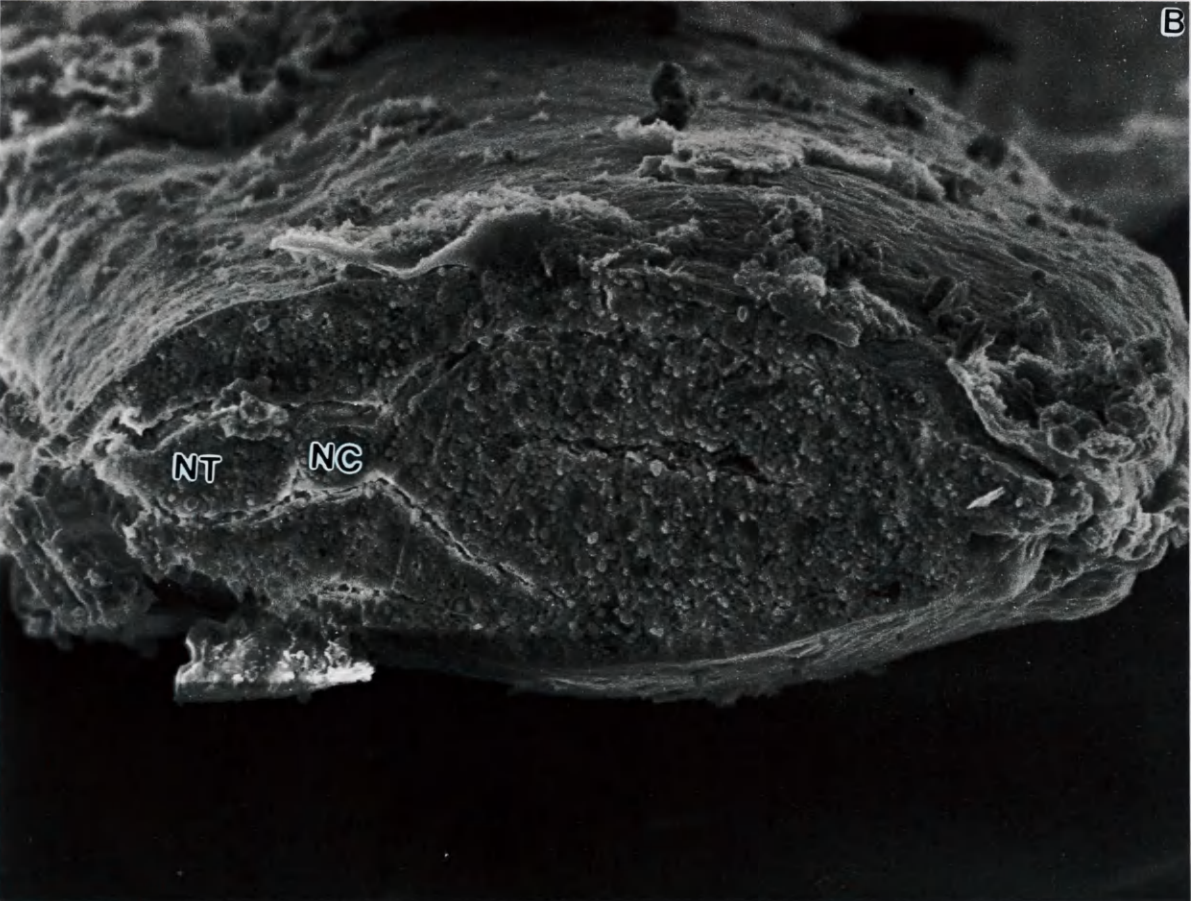
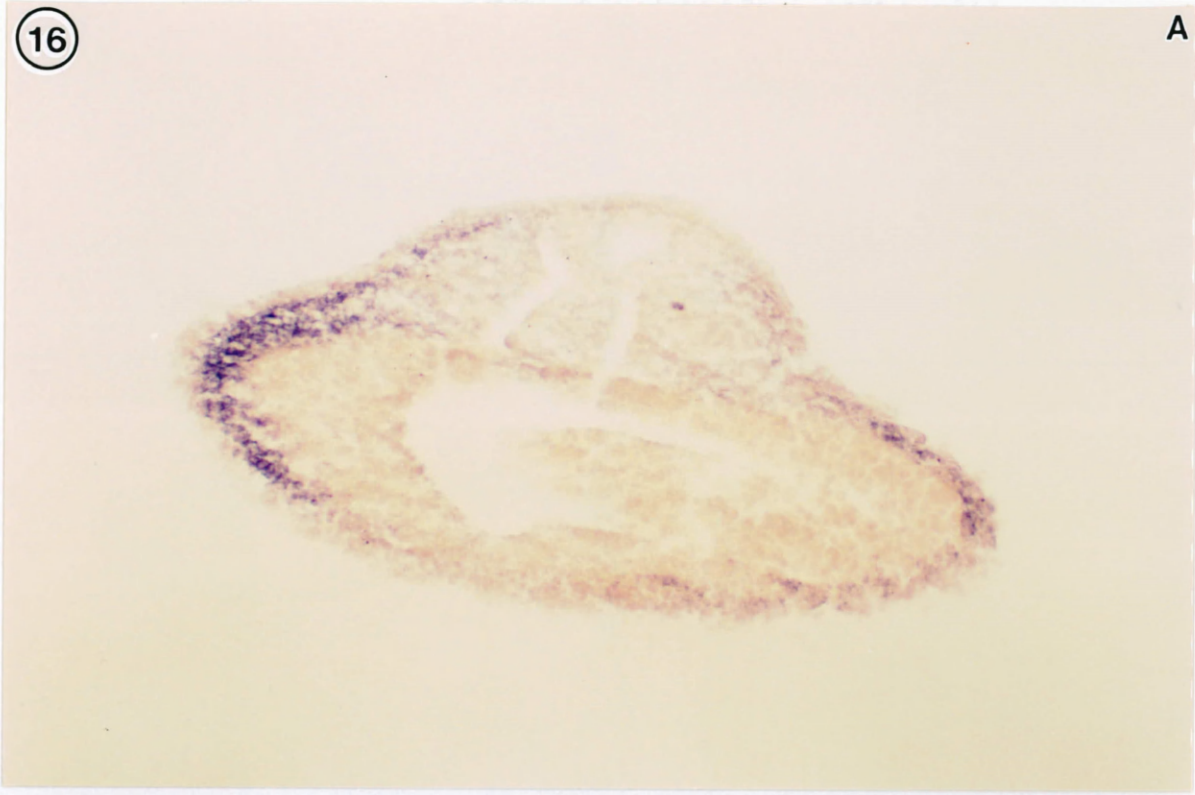


Figure 16. A transversely sectioned stage 25-27 embryo at 245 micrometers. (A) The segregation of the signal into the lateral mesoderm and the margin of the somitic mesoderm continues. The embryo has been compressed during sectioning and appears distorted, 100X. (B) In the SEM view there are morphological distinctions between the lateral mesoderm (LM) and endoderm (E), 112X.

16

A



B

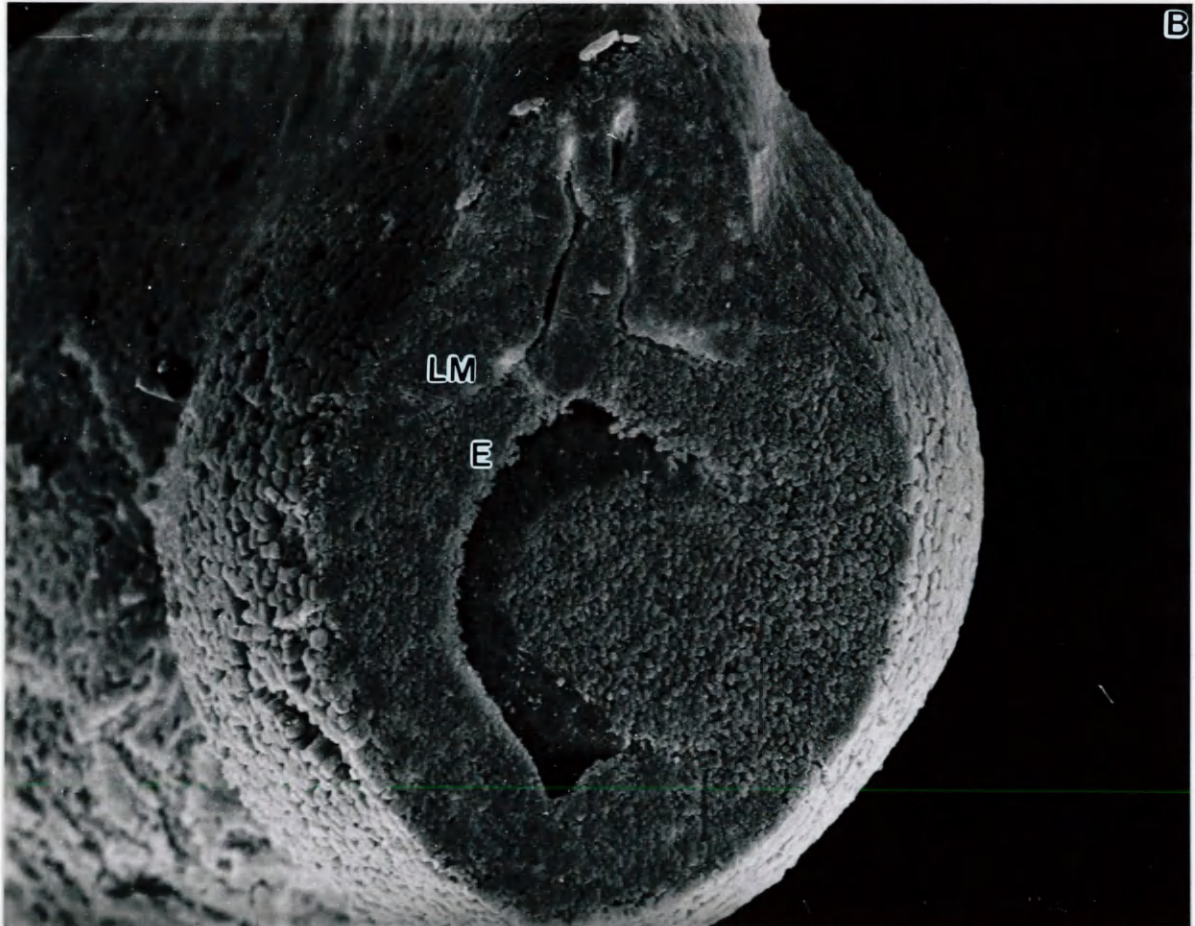
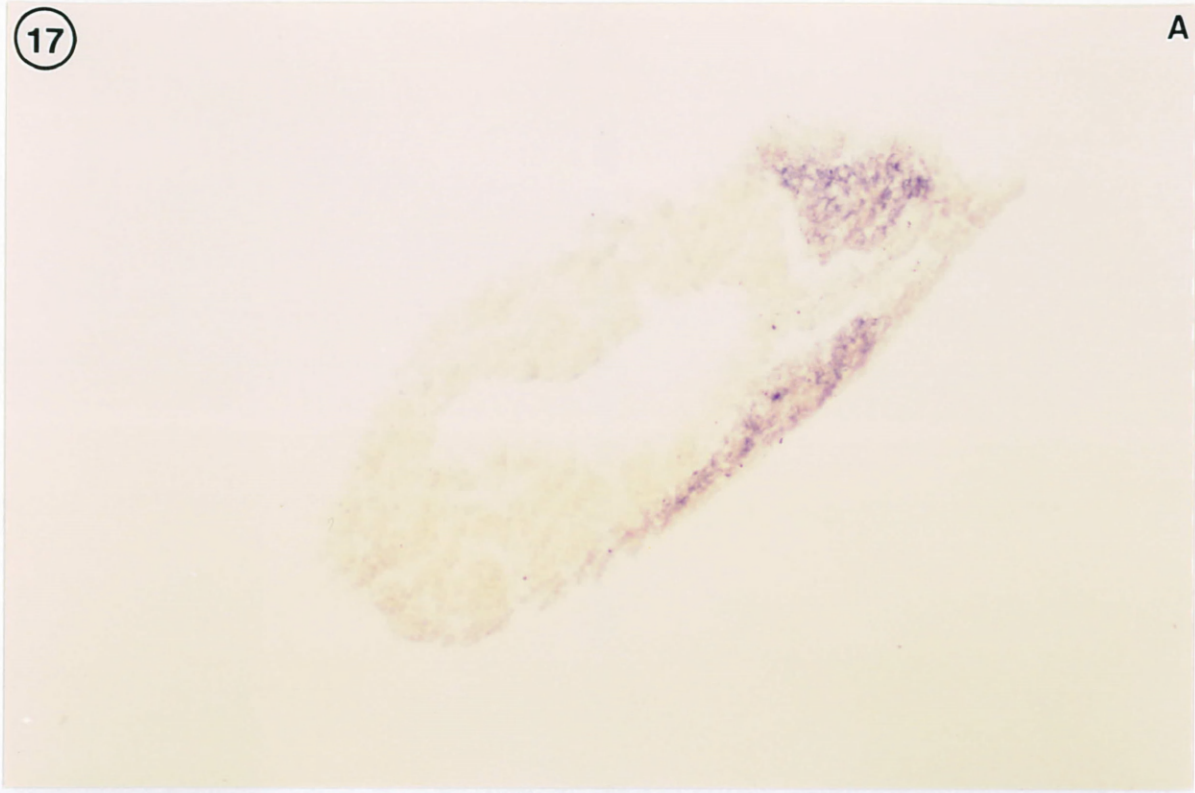


Figure 17. (A) At 280 micrometers into the tail of a stage 25-27 embryo the signal appears more strongly in the somitic mesoderm, 100X.(B) The embryo is sectioned to the level of the hindgut (HG), 115X.

17

A



B

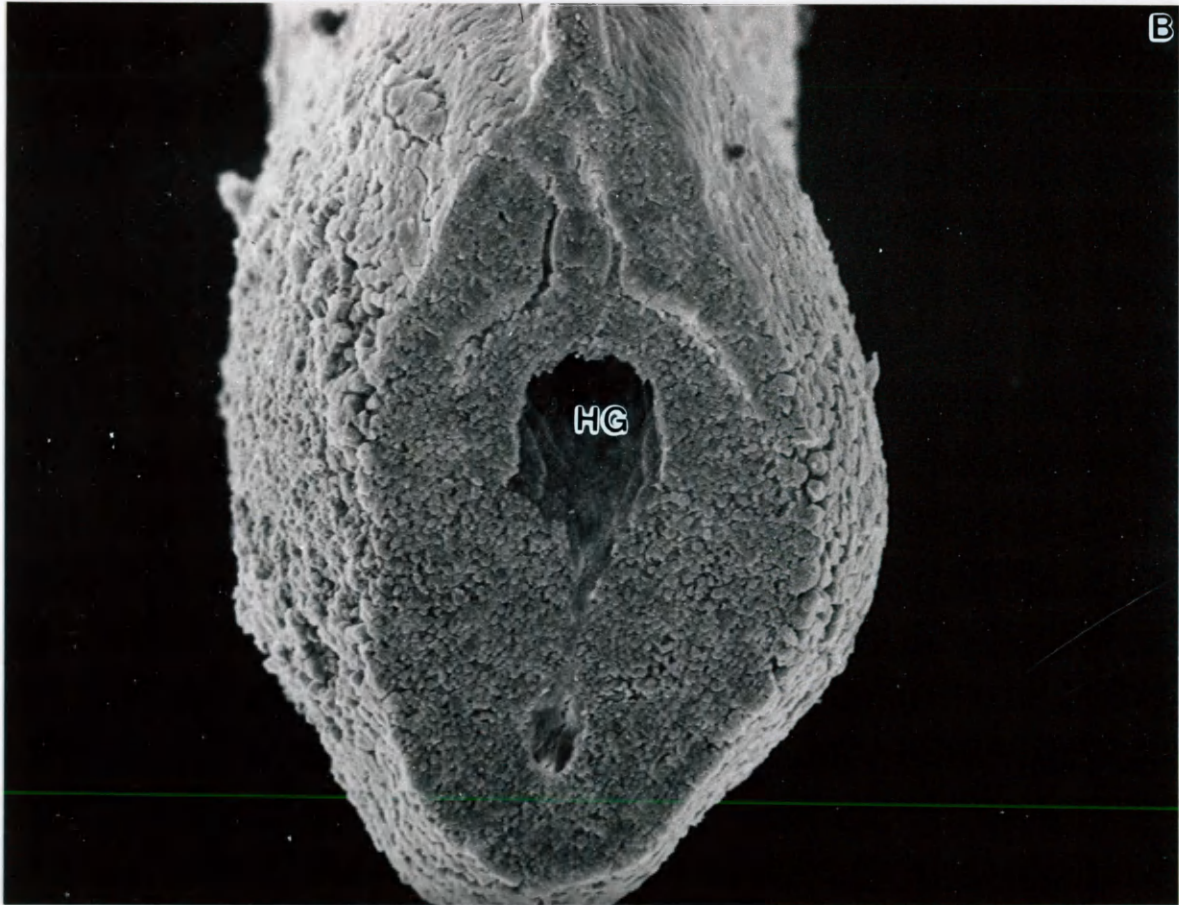
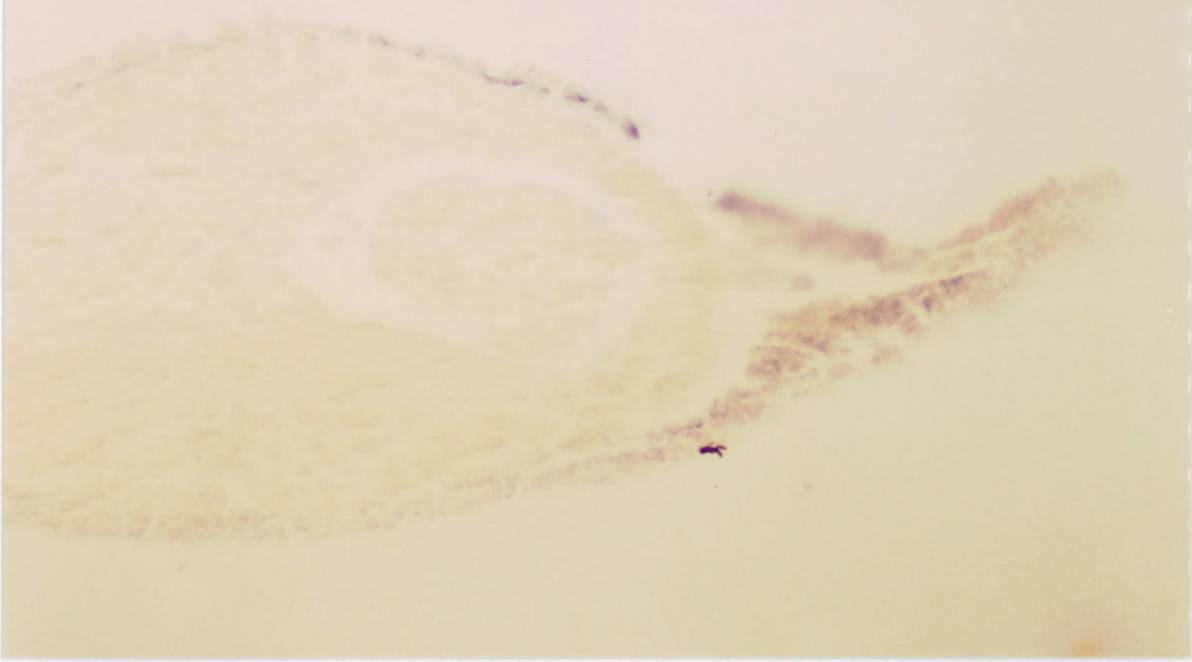


Figure 18. A stage 25-27 embryo. (A) Transverse sectioning to 315 micrometers reveals the signal continuing in the mesodermal tissues, 100X. (B) The band of lateral mesoderm (arrowhead) is becoming narrower as the differentiation of internal structures continues, 96X.

18

A



B

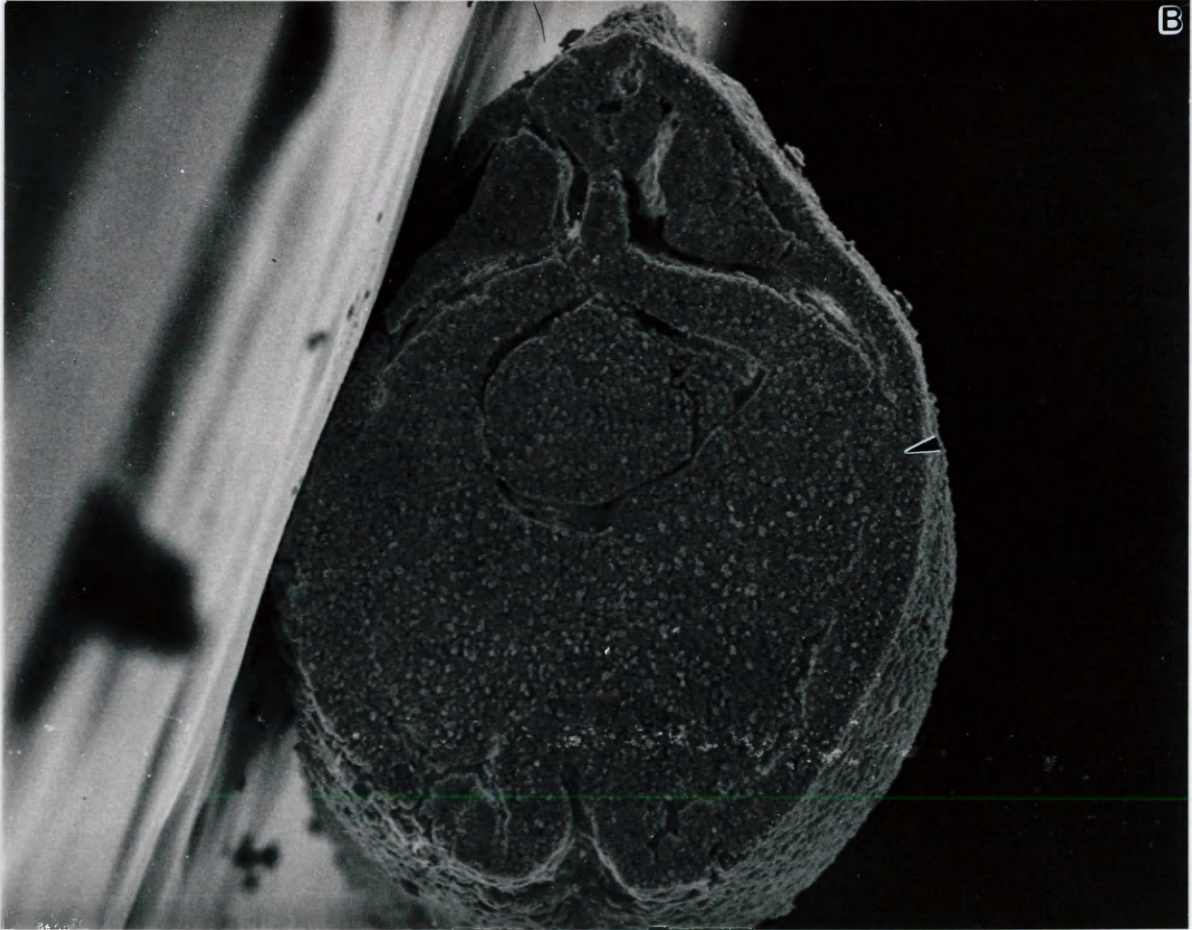
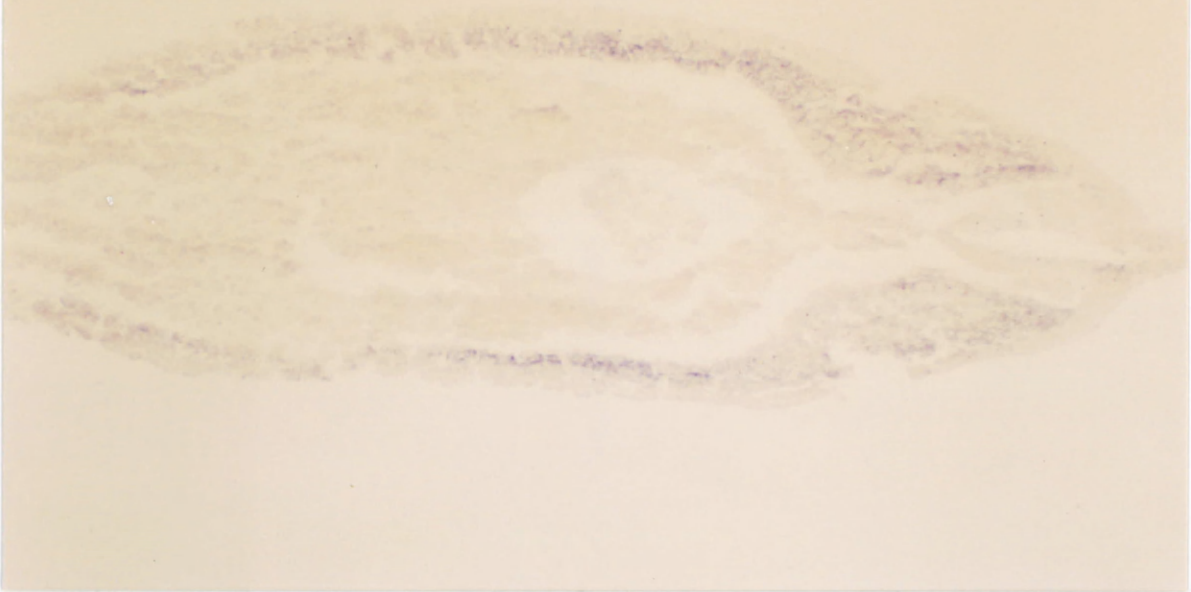


Figure 19. Transverse sectioning of a stage 25-27 embryo to 350 micrometers. The correlation between the LM and SEM views reveals some subtle differences in the morphology of the internal tissues. (A) The LM view of signal expression, 100X. (B) The mesodermal tissue (M) appears to have a flatter and more uniform surface while the endoderm (E) appears more granular, 85X.

19

A



B

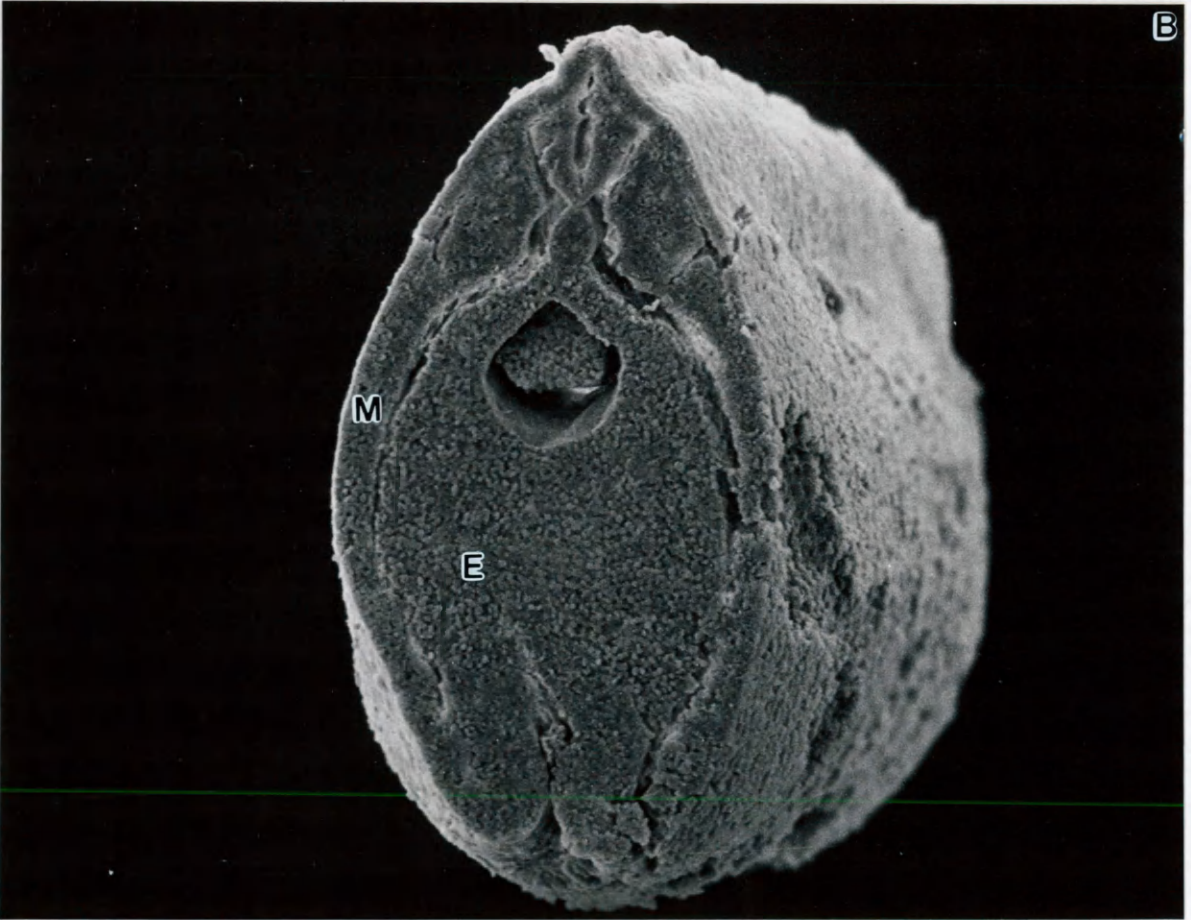


Figure 20. 420 micrometers into the tail region of a stage 25-27 embryo. (A) The signal of *XEGR-1* is now delimited to the lateral edges of the mesoderm (arrowheads), 100X. (B) The SEM view of the same embryo, 87X.

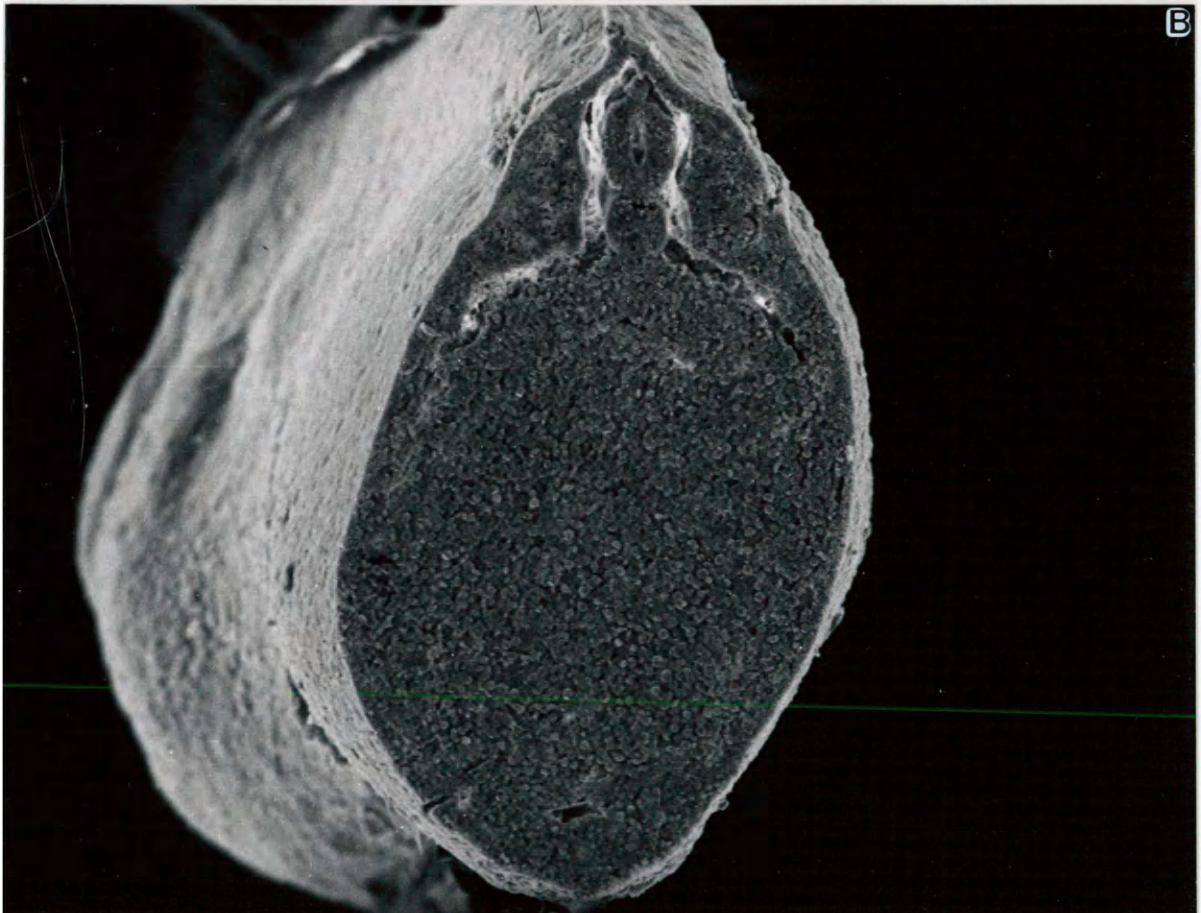


Figure 21. Transverse section of a stage 25-27 embryo to 525 micrometers (A) The expression of *XEGR-1* appears in a more punctate pattern in the lateral mesoderm (arrowheads), 100X. (B) The SEM view of the same embryo shows no differentiation in the tissues in the area of expression, 93X.

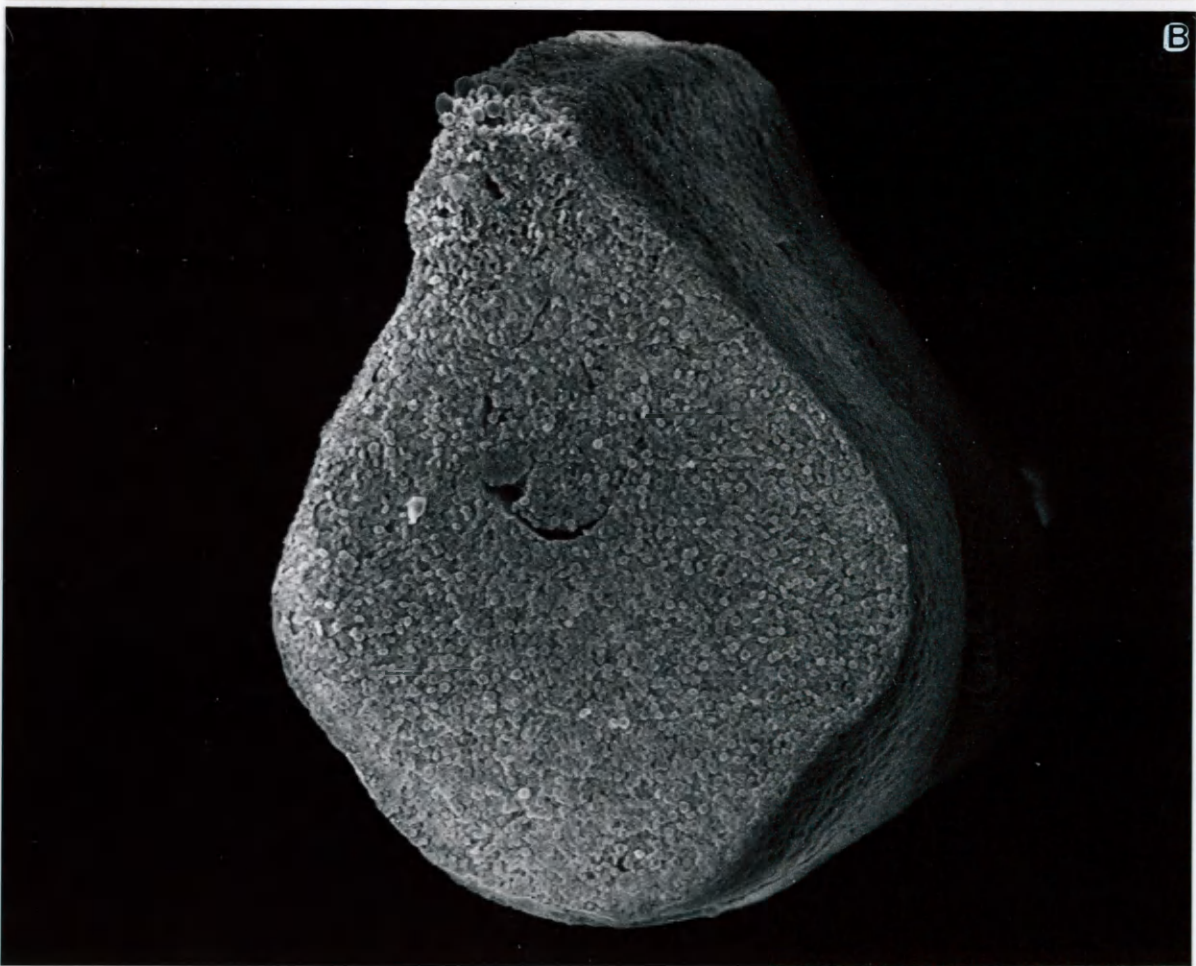
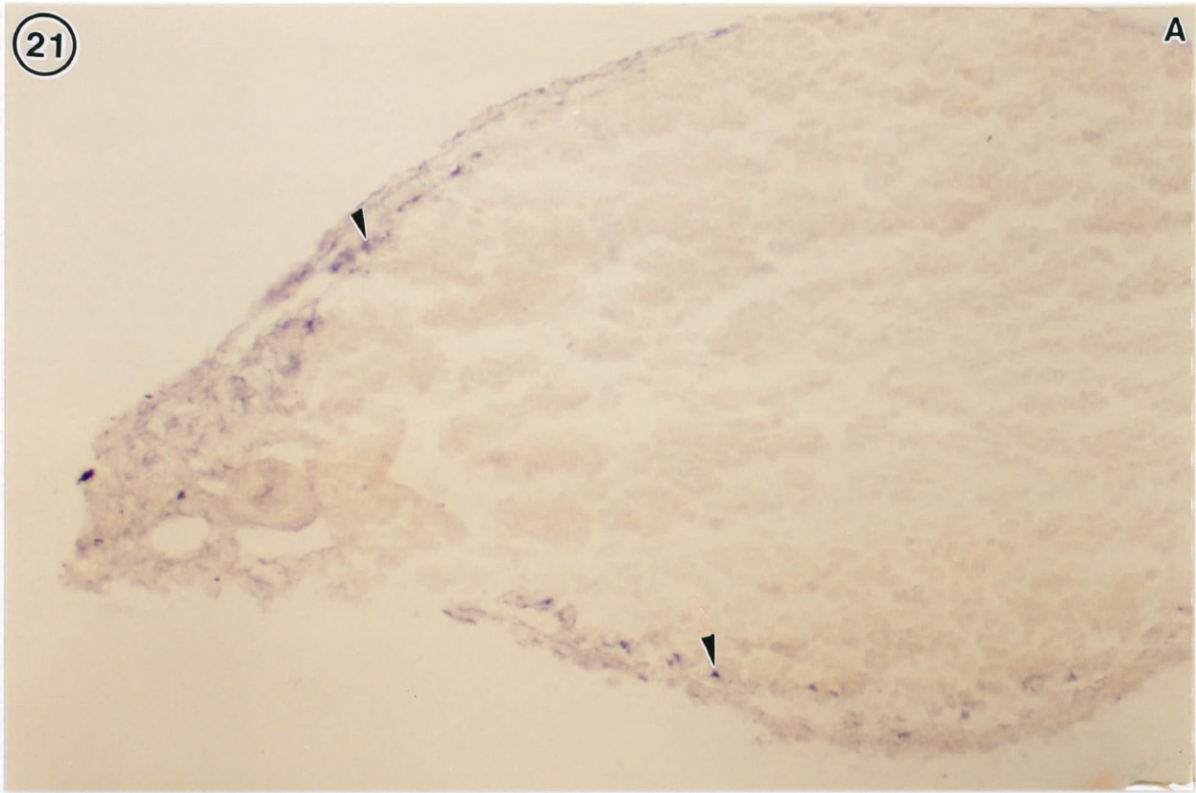


Figure 22. An LM/SEM correlated view of a stage 37 embryo. The embryo is longitudinally sectioned and viewed from the dorsal side. (A) After in situ hybridization *XEGR-1* expression appears in the tail bud (TB) region of the embryo, 100X. (B) The SEM view of the whole embryo, 26X. (C) A higher magnification view of the tailbud region focuses on the region of expression. The gene is expressed in the mesodermal tissue (M) but not the ectoderm (E), 123X (left) & 546X (right).

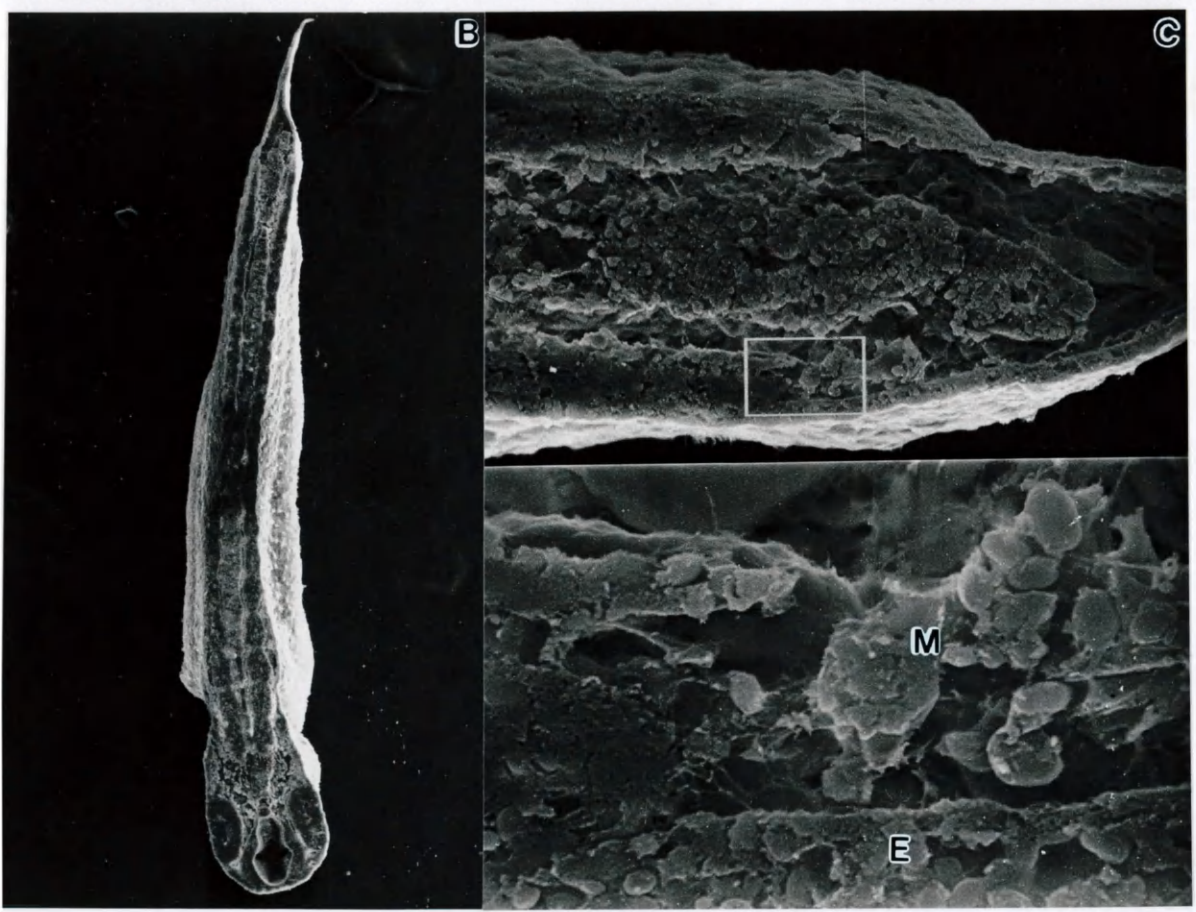


Figure 23. A transversely sectioned stage 37 embryo. (A) At 105 micrometers into the tail of the embryo signal is visible in the somitic and lateral mesoderm (arrowheads), 100X. (B) There are only slight morphological differences between the mesoderm and endoderm tissue despite the distinct pattern of signal expression, 108X.

23

A



B

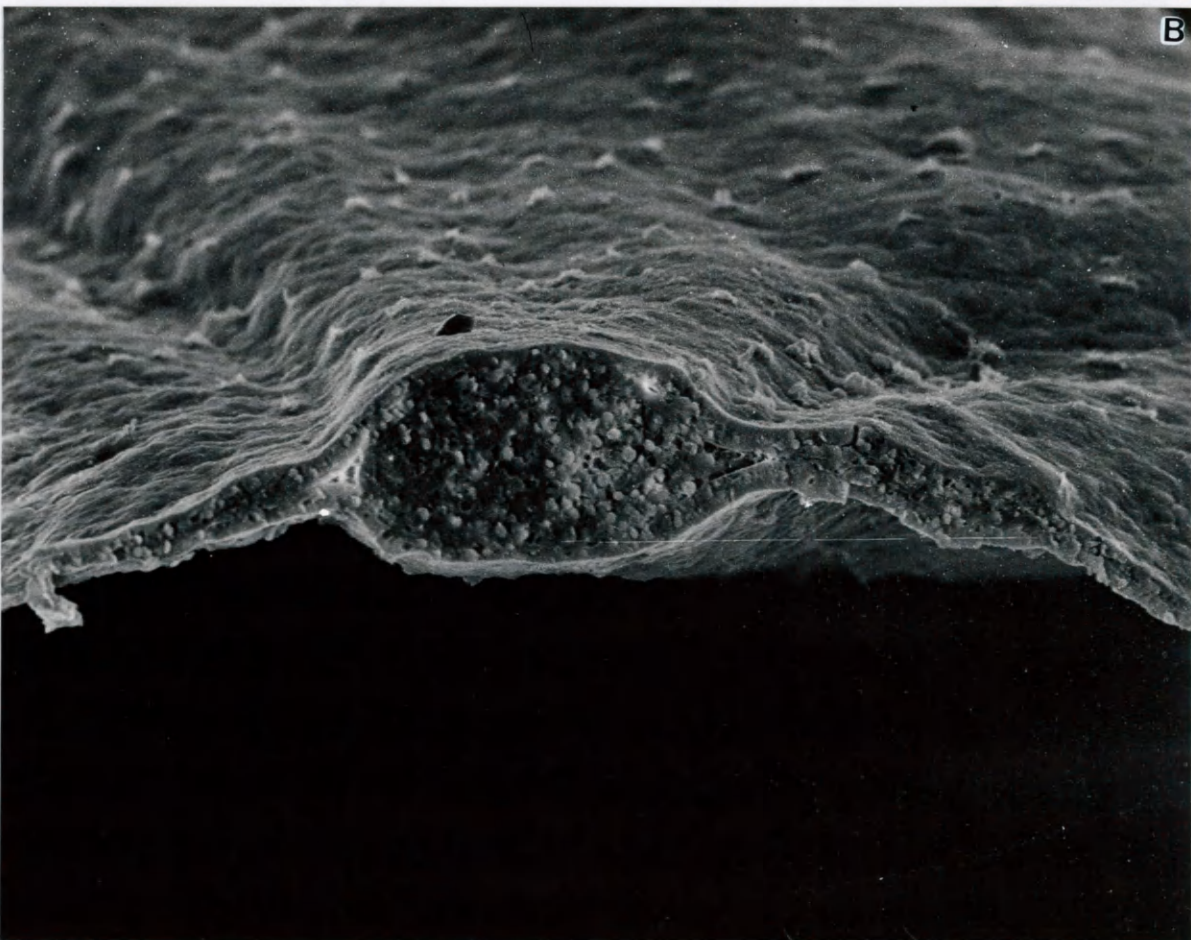


Figure 24. A stage 37 embryo transversely sectioned to 175 micrometers. (A) The signal appears very weakly in the mesodermal tissue, 100X. (B) The SEM view of the same embryo, 145X.

24

A



B

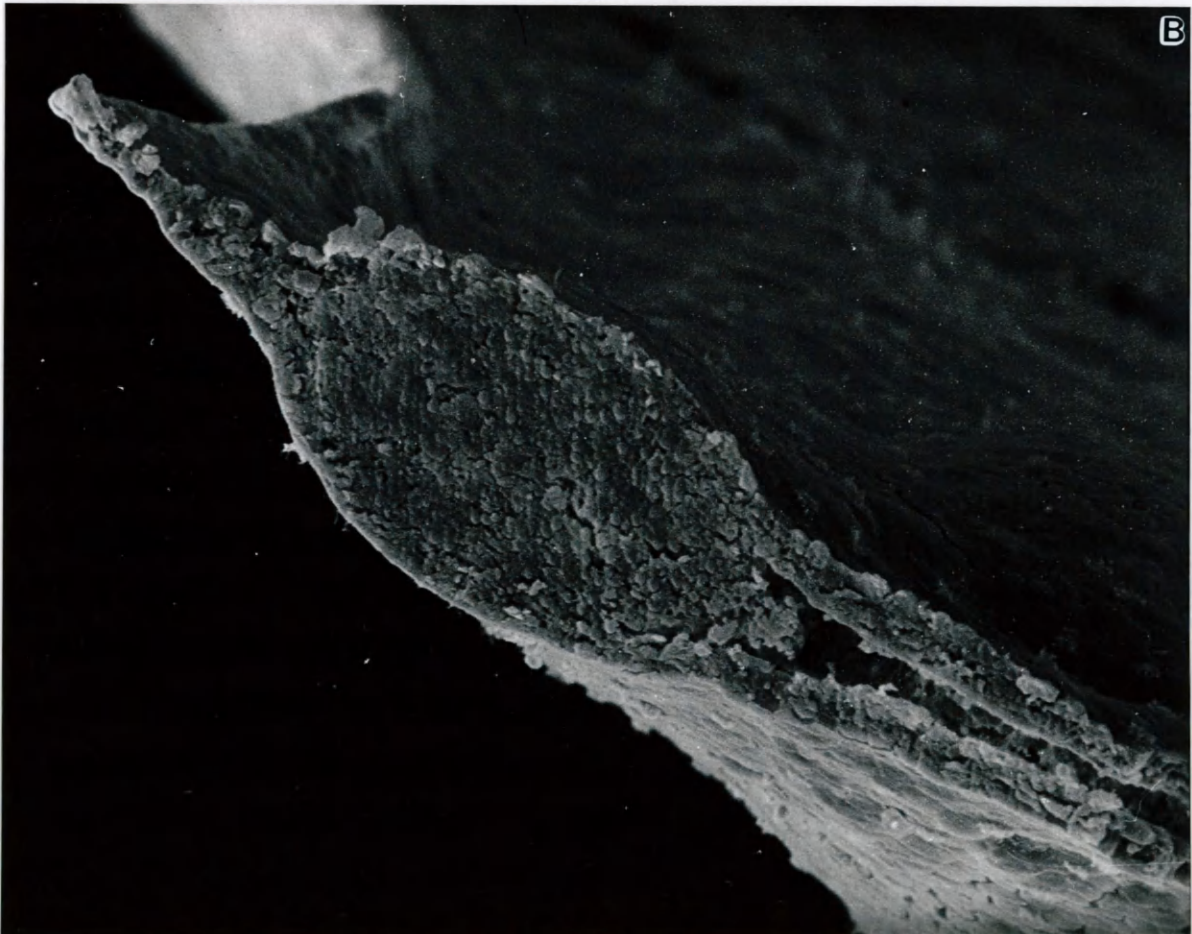
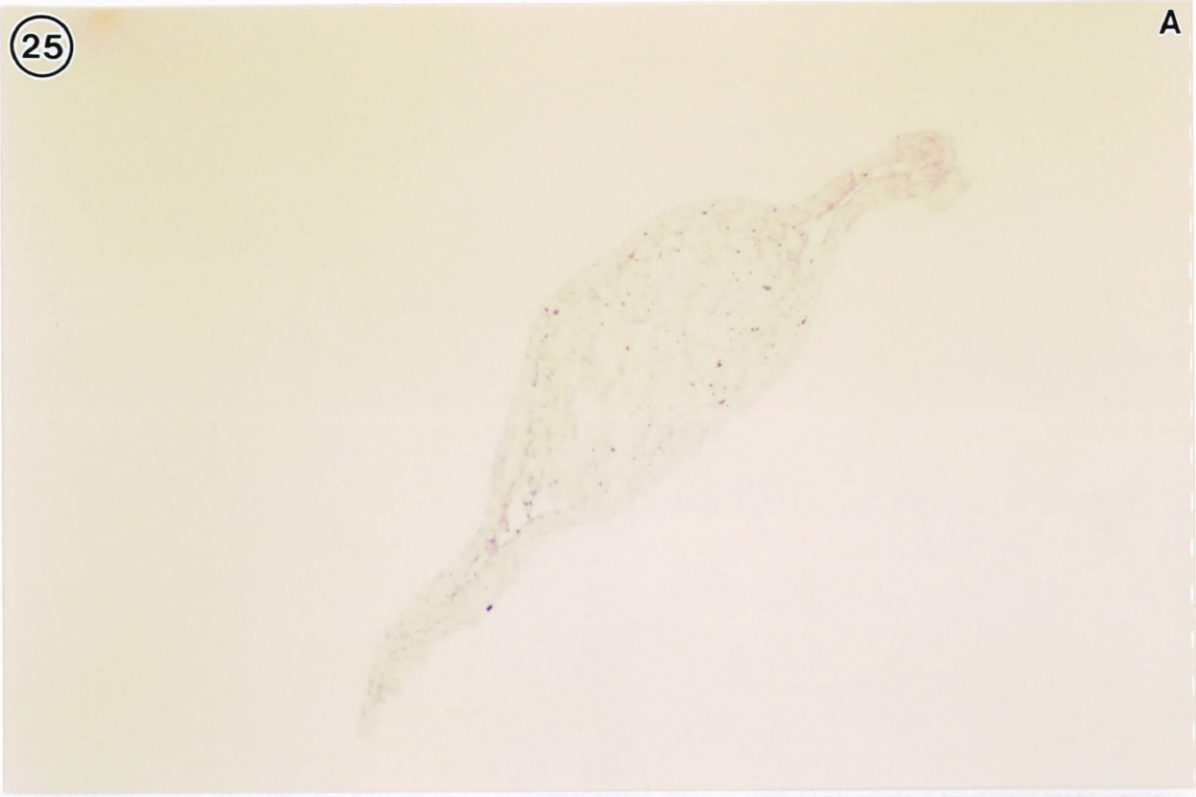


Figure 25. Transverse sections through a stage 37 embryo. At 245 micrometers differentiation of internal structures is apparent. (A) There is no longer any distinct signal visible in the mesodermal tissues after in situ hybridization, 100X. (B) The SEM view shows the neural tube (NT), notochord (NC) and somitic mesoderm (SM), 101X.

25

A



B

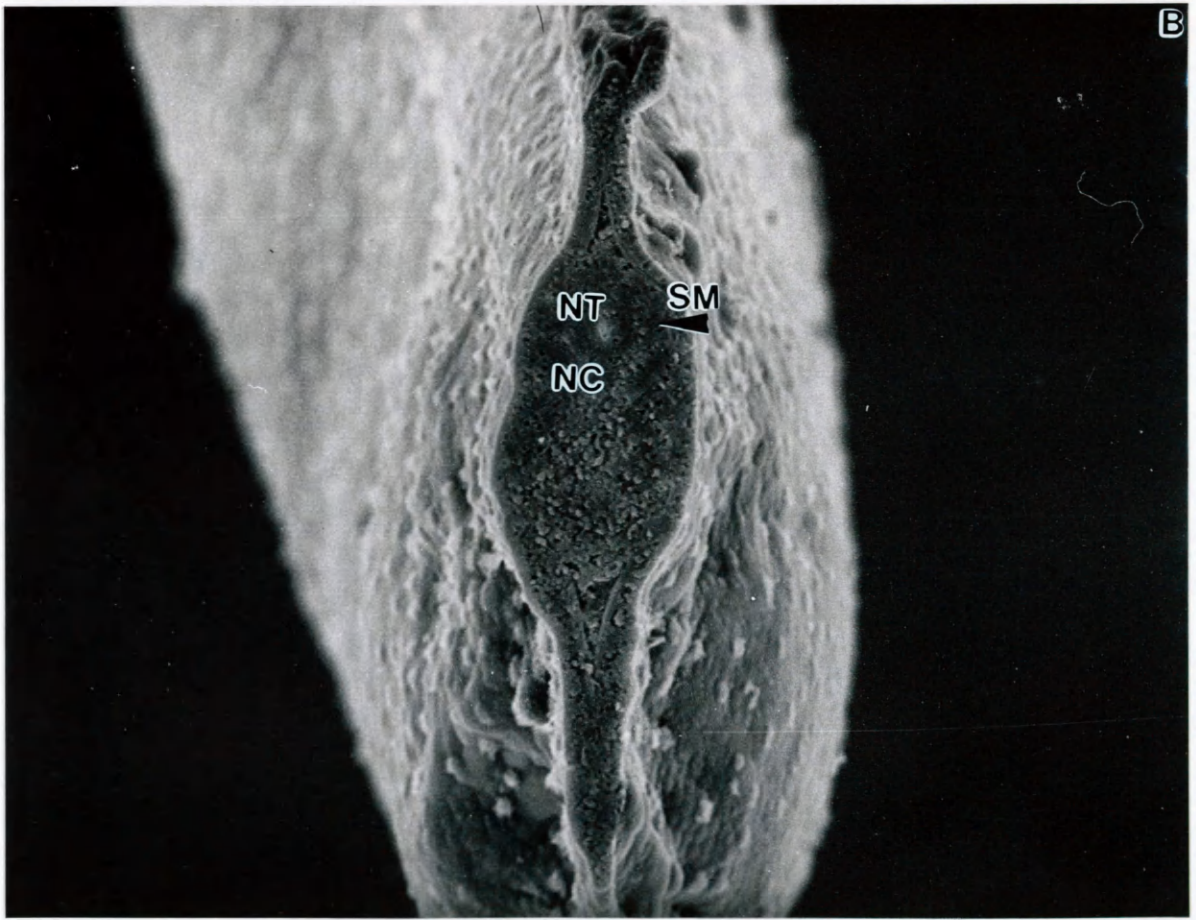


Figure 26. A stage 37 embryo transversely sectioned to 315 micrometers. (A) There is no distinct or strong signal present, 100X. (B) The micrograph shows the presence of somitic mesoderm (**SM**) flanking the neural tube, 106X.

26

A



B

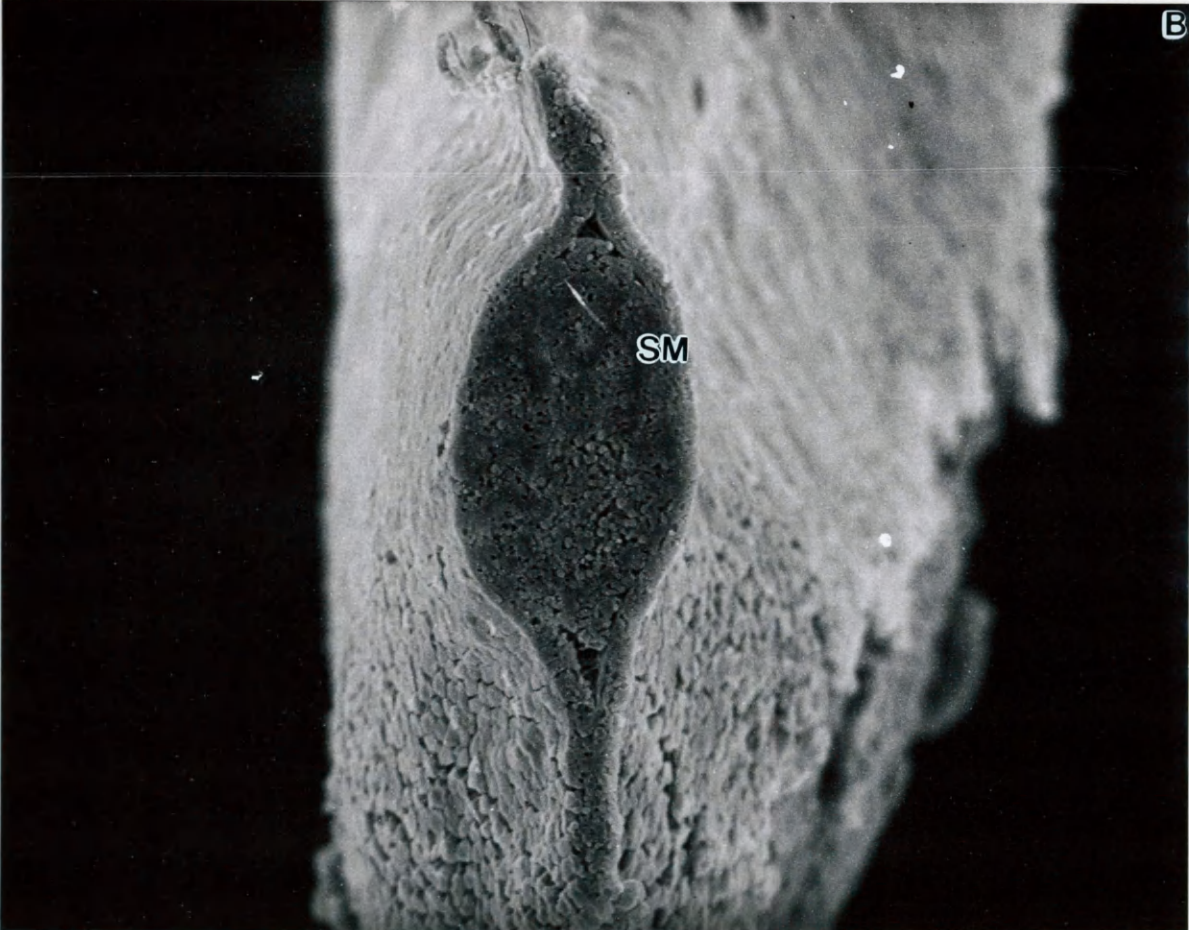
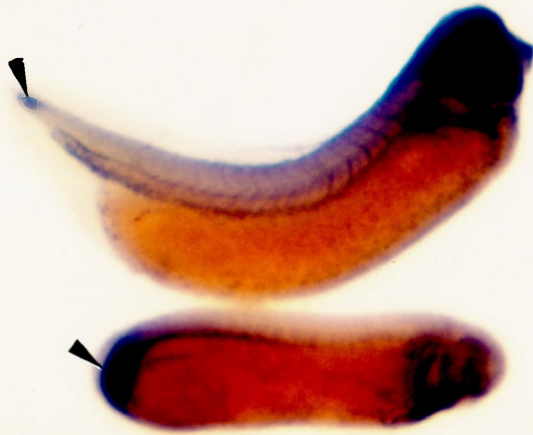


Figure 27. Whole mount in situ hybridization with *XEGR-1* using two labeling methods. (A) Stage 35 and stage 27 embryos, lateral view. The embryos have undergone a standard in situ hybridization using an alkaline phosphatase catalyzed signal. There is strong and very distinct signal in the tail region at both stages (arrowheads), 10X. (B) Stage 37 and stage 35 embryos, lateral view. The embryos have undergone in situ hybridization using a colloidal gold labeled probe. Visualization of the signal is achieved following a silver enhancement reaction leaving a gray to brown residue. Signal is again present in the tail region of the embryos (arrowheads), 10X.

27

A



B

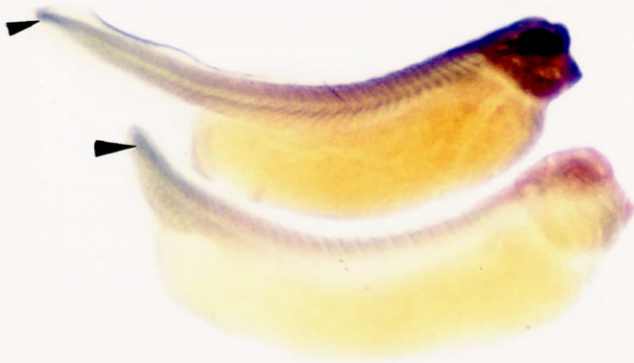
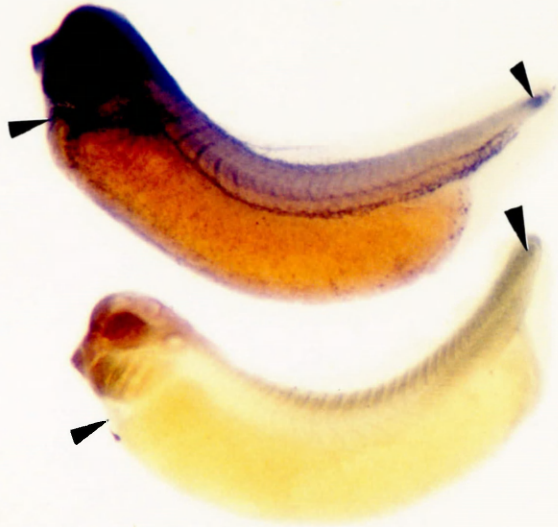


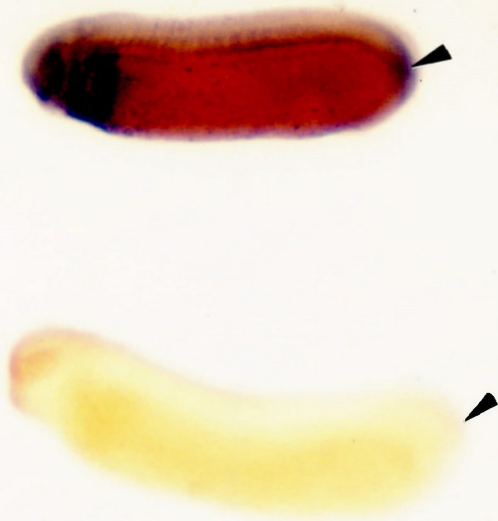
Figure 28. A comparison of whole mount embryos after *in situ* hybridization using two different labeling methods. (A) Stage 35/36 embryos show similar signal patterns (arrowheads) in whole mount *in situ* hybridization using the standard color reaction (top) and silver enhancement of colloidal gold (bottom), 10X. (B) Stage 25-27 embryos in the same orientation show some correlation of signal in the tail region (arrowheads), but the pattern is not as distinct in the younger embryos, 10X.

28

A



B



VITA

Laura Rochmis

Born in Washington, D.C., June 25, 1970. Graduated from James Madison High School in Vienna, Virginia, June 1988. Received a B.A in History from The College of William and Mary, June, 1992. Worked full time in 1992-93 before entering the biology graduate program at William and Mary in 1993. Will begin the first year at Eastern Virginia Medical School in the fall of 1995.